INL/EXT-18-51416-Revision-0

ATF Transient Prescription Tests in TREAT

Benjamin A Baker, James R Parry, Tommy V Holschuh, Cliff B Davis, Javier Ortensi, Mark D DeHart, Nicolas E Woolstenhulme, Daniel M Wachs, Connie M Hill

September 2018

The INL is a U.S. Department of Energy National Laboratory
operated by Battelle Energy Alliance

INL/EXT-18-51416-Revision-0

ATF Transient Prescription Tests in TREAT

Benjamin A Baker, James R Parry, Tommy V Holschuh, Cliff B Davis, Javier Ortensi, Mark D DeHart, Nicolas E Woolstenhulme, Daniel M Wachs, Connie M Hill

September 2018

Idaho National Laboratory
Idaho Falls, Idaho 83415

http://www.inl.gov

Prepared for the
U.S. Department of Energy

Under DOE Idaho Operations Office
Contract DE-AC07-05ID14517

INL/EXT-18-51416
Revision 0

ATF Transient Prescription Tests in TREAT

Nuclear Technology Research and Development

Prepared for
U.S. Department of Energy
Advanced Fuels Campaign

Benjamin Baker, James Parry, Thomas Holschuh, Cliff Davis, Javier Ortensi, Mark DeHart, Nicolas Woolstenhulme, Daniel Wachs, Connie Hill
INL National Laboratory

September 2018
NTRD-FUEL-2017-000059

EXECUTIVE SUMMARY

The Transient Reactor Test (TREAT) facility was constructed in the late 1950s and provided thousands of transient irradiations before being placed in standby mode in 1994. In 2017, it resumed operation in order to reclaim its crucial role in nuclear-heated safety research. TREAT is a transient reactor where inherently-safe core physics, a nimble transient rod drive system, and a philosophy of continual facility improvement work together to enable flexible power maneuvers for fuel safety research. While the facility's flexible design and multi-mission nature saw historic experiments for numerous transient types, TREAT was not specifically adapted to optimize or demonstrate its full performance capability for Light Water Reactor (LWR) postulated accidents including Hot Zero Power Reactivity Initiated Accidents (HZP-RIA) and Loss of Coolant Accidents (LOCA).

The physics of HZP-RIA drive very brief pulses with fairly large energy excursions. TREAT is currently capable of approaching HZP-RIA pulse widths through transients initiated on a large step insertion of reactivity and terminated shortly thereafter by rapid re-insertion of the transient rods ("clipping"). LOCAs are postulated to occur quite differently, starting from normal power operations followed by a long period of lower power decay heat. TREAT is able to simulate LOCA events with an initial flattop transient for tens of seconds, followed by a sizeable power reduction, to a longer segment where specimen fission heating represents internal decay heat generation.

Two reactor physics testing campaigns were undertaken to address the HZP-RIA type transients, neither of which had been performed in any great measure historically to address data gaps in the timing, repeatability of clipping, and effect of dynamic transient rod motions on core-to-specimen fission power coupling. The first campaign, referred to as the Accident Tolerant Fuel (ATF) transient prescription tests, employed dosimeters in the core to characterize the effect of rod motions on specimen power coupling for clipped, unclipped, and low-level steady state operations each with approximately the same moderate core energy release. This campaign was accompanied by efforts to measure dosimetry and compare results to analytic predictions. The other HZP-RIA campaign, referred to as Narrow Pulse Width (NPW) transient prescriptions, employed higher step insertions with increased core energy release to demonstrate TREAT's capability in achieving the narrowest-possible pulse width. Additionally, a series of LOCA transient prescriptions were also performed to demonstrate how well TREAT could perform long-duration shaped transients. Both NPW and LOCA transient prescriptions did not include dosimeters but used existing plant power instrumentation to produce transient power data.

All three transient prescription campaigns were successfully carried out in TREAT. The ATF-3 transient prescriptions showed that TREAT can perform clipped transients with remarkable repeatability. Measurement and modeling both showed that the power coupling in small, fissile dosimeters does not change by more than 8% between clipped, unclipped, and steady state runs while uncertainty sources in both the modeling and measurement methods were identified and found to be on the order of 20% in total. Overall, the ATF-3 transient prescription tests were successful in determining repeatability and consistency of dosimeter power coupling, developing processes for modeling and measuring this crucial parameter, and demonstrating the need for continued efforts in transient prescription work at TREAT in support of future experiment design and post test data interpretation.

The NPW and LOCA transient prescriptions were also successfully performed to exhibit TREAT's capability for these important LWR accident categories. The NPW transients showed pulse widths of ~90 ms, which were the narrowest ever achieved in TREAT to date and relevant for the upper end range of HZP-RIA simulation. This effort provided crucial data for calibrating kinetic models to be used in enhanced pulse-narrowing strategies in upcoming irradiations. Similarly, The LOCA transient prescriptions showed that TREAT can simulate the needed nuclear heating and event time scales for LOCA fuel safety research and provided essential data for future experiment design.

INTENTIONALLY BLANK

CONTENTS

FIGURES

TABLES

INTENTIONALLY BLANK

1. INTRODUCTION

The Transient Reactor Test (TREAT) facility was constructed in the late 1950s and provided thousands of transient irradiations before being placed in standby mode in 1994. In 2017, it resumed operation in order to reclaim its crucial role in nuclear-heated safety research. TREAT is an air-cooled reactor, driven by a core of graphite blocks, having a small concentration of dispersed uranium oxide. TREAT's fast-acting hydraulically-driven transient control rods are coupled with the Automatic Reactor Control System (ARCS) to leverage the core's negative temperature feedback and enable unrivaled power shaping capability. TREAT is a transient reactor where inherently-safe core physics, a nimble transient rod drive system, and a philosophy of continual facility improvement work together to enable flexible power maneuvers relevant to current-fleet nuclear plants, advanced reactors, and scientifically-valuable power shapes. While the facility's flexible design and multi-mission nature saw historic experiments for numerous reactor fuels and transient types, TREAT was not specifically adapted to optimize or demonstrate its full performance capability for Light Water Reactor (LWR) postulated accidents including Hot Zero Power Reactivity Initiated Accidents (HZP-RIA) and Loss of Coolant Accidents (LOCA).

The design basis for HZP-RIA is a postulated accident in commercial LWR plants initiated by ejection of control elements (e.g., control rods/blades) from the core after it has been pressurized and preheated but before it is producing significant fission power. The physics of HZP-RIA drive brief pulses with fairly large energy excursions. During this time, excursion fuel pellets can heat and expand rapidly into mechanical interaction with the relatively cold cladding. The cladding's time, temperature, and stress response is chiefly driven by the energy deposited in the pellet and the duration of this pulse in these scenarios. While TREAT cannot currently provide pulse durations as brief as desired, it is currently capable of approaching HZP-RIA pulse widths through transients initiated on a large step insertion of reactivity and terminated shortly thereafter by rapid re-insertion of the transient rods ("clipping").

LOCAs are postulated to occur quite differently, starting from normal power operations in pressurized water conditions, followed by a major breach of the primary coolant system pressure boundary. Such an event then results in rapid depressurization so that water changes to steam roughly coincident with a reactor shutdown (via SCRAM and/or loss of moderator). Fuel rods surrounded by steam then experience a long period of fuel rod overheat due to decay heat before liquid water reenters and quenches the fuel. TREAT is able to simulate the nuclear heating conditions of a LOCA with an initial flattop transient for tens of seconds, followed by a sizeable power reduction, to a longer segment where low-level specimen fission heating represents internal decay heat generation.

Two reactor physics testing campaigns were undertaken to address the HZP-RIA type transients. This type of "prompt pulse fast clip" transient was not performed in any great measure historically. As a result, two large data gaps must be addressed including: 1) timing repeatability of clipping (which has a marked effect on core energy release) and 2) the effect of dynamic transient rod motions on core-to-specimen fission power coupling. The first campaign, referred to as the Accident Tolerant Fuel (ATF) transient prescription tests, employed dosimeters in the core to characterize the effect of rod motions on specimen Power Coupling Factors (PCF) and Transient Correction Factors (TCF) for clipped, unclipped, and low level steady state operations, each with approximately the same moderate core energy release. [1] This campaign was accompanied by efforts to measure dosimetry and compare results to analytic predictions; comprising the majority of the work reported herein.

The other HZP-RIA campaign, referred to as Narrow Pulse Width (NPW) transient prescriptions, was performed later and employed higher step insertions with increased core energy release to demonstrate TREAT's capability in achieving the narrowest-possible pulse widths. [2] These transients were essentially a demonstration of reactor capability as indicated by plant instrument and did not include dosimeters, primarily because the primary dosimeter material (uranium metal fission wire) was predicted to melt during the higher energy irradiation. The outcomes from this effort were also purposed to calibrate kinetic models and enable refined design of future experiments and ongoing projects with the aim to deploy further pulse-narrowing strategies.

Finally, a series of LOCA transient prescriptions were performed which, like the NPW tests, used plant instrumentation to demonstrate how well TREAT could perform long-duration shaped transients. [3] Again, dosimeters were omitted due to the high core energy release. The resulting LOCA test data were purposed for input to concurrent experiment designs, including capsules and loops, with the ability to create LOCA-like thermal hydraulic boundary conditions for fuel specimens.

All of these transient prescription campaigns were performed using the M8-CAL vehicle in the M8 half-slotted core configuration since this core configuration was well-characterized historically and was used in TREAT's initial physics testing campaign. While the M8 core configuration will not exactly match all future LWR test scenarios in TREAT, the fundamental physics of interest were thought to be adequately represented by the planned core and selected transients.

2. ATF-3 TRANSIENT PRESCRIPTION TESTS, BASELINE INFORMATION

The modeling efforts for the ATF 3-1 transient prescription focuses on fission wires used in one low level steady state (LLSS) irradiation and two transients as outlined in the ATF 3-1 Transient Prescription Data Package (DP-125). [1] The details of the reactor runs are listed in Tables 1-2 below. Table 3 shows details of the fission wires. All of these runs are to be performed in the M8 calibration vehicle which was left in the reactor when TREAT was shut down in 1994. The description of the vehicle can be found in Ref [4].

Table 1. LLSS characteristics.

Power Level (kW)	Duration (hours)	Maximum Energy Released (MJ)
80 ± 10	2	600

Table 2. Transients to model.

Reactivity Insertion (% Δk/k)	Estimated Reactivity Insertion ($)	Transient Type	Estimated Total Energy Released (MJ)
1.50 ± 0.1	2.09 ± 0.14	Natural	576
2.60 ± 0.1	3.62 ± 0.14	Clipped	587

Initially, it was understood that the U235 concentration was near 0.36 wt% but was unverified. The value was measured, and results were obtained after the experiments had taken place. The measured estimates indicated the enrichment was ~0.2 wt% [5-7]. Due to scheduling and time availability, the initial phases of the modeling efforts were performed before the enrichment value was measured and was assumed to be 0.36 wt%. Further, the wire was assumed to be round, which turned out to be incorrect [8]. This fact did not influence the modeling portion of this paper, but it did influence the experimental values by means of a correction that is calculated from modeling the fission wire for the percentage of photons that never leave the wire.

Table 3. Fission wire.

Alloy	U Enrichment (wt% 235U)	Diameter mm	Length mm
Depleted Uranium (DU) (Initial Estimate)	0.36	1.59	5
Depleted Uranium (Measured)	~0.2	N/A Ref [8]	Ref [9]

Figure 1 shows the positioning of the fission and flux wires within the M8 calibration vehicle. While observing Figure 1, it is important to note that there are Dysprosium (Dy) collars, which are in the form of a stair step around the vehicle. Dysprosium is a strong neutron absorber, and its original purpose was to eliminate the thermal spectrum for fuel from the fast spectrum reactor Experimental Breeder Reactor II (EBR-II). As a figure of merit, the Dy collars are worth about the same as one of the control rod drives in TREAT.

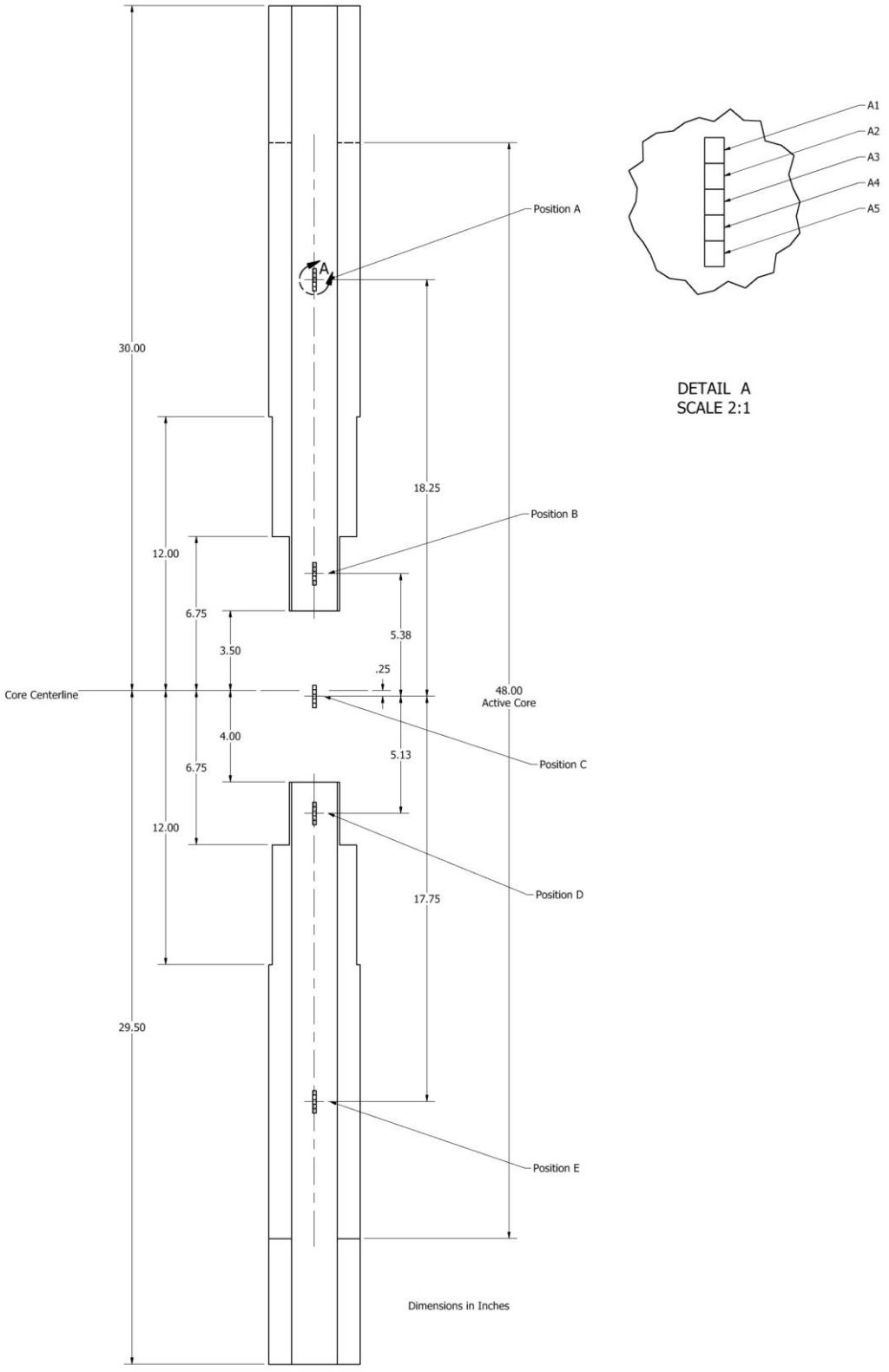

Figure 1. Flux and fission monitor wire locations.

3. ATF-3 TRANSIENT PRESCRIPTION TESTS, MODELING EFFORTS

This section will discuss the desired outcomes from the modeling efforts, modeling methods, and assumptions and/or approximations.

3.1 Desired Outcomes

Ultimately, an experimenter would like to know how much and at what rate energy will be deposited in the experiment during a given transient. However, the best measurement of this can only be best estimated after performing the transient on the fuel specimen of interest. Since most of the fuel specimens require millions of dollars to prepare and specimens might reach melting conditions, it is desirable to get a fairly good handle on the outcome before the experiment is ever performed.

To address this issue, TREAT in the past has performed a series of calibration irradiations and transients with much less expensive fission wires. After the irradiations and transients, the integral fissions are measured to determine the amount of energy put into the fission wire. Additionally, integral fissions can be measured from LLSS irradiations of a fuel specimen where it is guaranteed to not melt. From the fission wire measurements and the results of the fuel specimen at LLSS, ratios can be used to estimate the energy that will be deposited in the fuel specimen for a transient. This method relies on a critical assumption that the ratio of the transient results to steady state results for the fission wire are the same for the fuel pin. The ratios that are developed from the fission wires and/or LLSS irradiations are used to create the power coupling factors (PCF) or transient coupling factors (TCF) or energy coupling factors (ECF). The units vary depending upon the application, but commonly used units are fissions per gram (f/g) in the sample per mega-watt (MW) in the core or Joules per gram (J/g) in the sample per mega-joule (MJ) in the core. The essence of these units is to describe something related to energy in the sample versus the reactor as a whole.

In practice, the fissions per gram or Joules per gram units come from measurements of the fissile material after an irradiation or transient using decay of fission products, which indicates the total number of fissions in the sample. The mass unit can easily be measured with scales and, typically, has much lower uncertainty. The energy from the core is calculated two ways depending on the mode of operation. For a transient, the energy in the core is estimated based on the integration of electrical charge in 3 linear uncompensated ion chambers. For LLSS runs, operators manually report the energy by estimating the power multiplied by time. Much discussion is needed to explore the variation and uncertainty that results from the energy in the core term. The variation in these measurements will be explored further, but, for now, it is important to understand how the data are experimentally determined and that the PCF values come from the aggregate of these independent measurements.

The overall goal of the transient prescription was to determine if the PCFs change significantly depending on the run history and how repeatable the runs are. The desired modeling outcomes were to compare measurable results with calculated results, with an emphasis around the PCFs or quantities that make up the PCF and to investigate best practices along with modeling accuracy.

3.2 Modeling Methods

In order to model the resultant PCF or reaction results, a series of calculations from different codes was required. Most of the modeling methods hinge on the use of a Monte Carlo calculation. Monte Carlo calculations are stochastic type codes based on using random numbers and probability distributions of cross sections to simulate the random behavior of neutron histories. Monte Carlo methods are only considered correct after a sufficient number of neutron histories have been performed for the quantity of interest. In addition, multiple Monte Carlo computations are required to obtain a true population statistic. The advantage of Monte Carlo is that it uses very few approximations to solve the transport equation. However, the disadvantage of Monte Carlo methods is that they are limited to steady state or fairly simple time-dependent calculations and limited on their coupling with other physics. Conversely, deterministic

methods solve the partial differential equation of the transport equation. The disadvantage of deterministic methods is that they include more approximations (i.e., few groups), and discretization error. Deterministic codes can vary in complexity from point-kinetics, in which only the time dependence is treated or diffusion, which retains the energy, time and space dependence, to very complex 3-D transport problems with energy, angular, spatial and time dependence. However, it would be very computationally expensive, even with today's computing power, to solve a full transport time-dependent problem for a full core. The solution is to use a mixture of codes to perform calculations and identify the most important variables. The process and codes used will change depending on the experiment at hand.

In addition to using different codes for each step, multiple codes were used for the same step to reveal potential differences. As well, different paths are possible. The codes that were used for the Monte Carlo method are Monte Carlo Neutron Particle (MCNP) and Serpent. MCNP was developed by Los Alamos National Laboratory and stems from the Manhattan project. Serpent was developed by VTT Technical Research Center of Finland starting in 2009. The deterministic codes used are: RELAP5-3D, S-TREK and MAMMOTH. [10] RELAP5-3D and S-TREK are both used for the point-kinetics modeling. MAMMOTH is a MOOSE-based application, which uses the Rattlesnake [11] deterministic transport solver to obtain solutions to various discretizations of the transport equation, from point kinetics to spherical harmonics and discrete ordinates. One of the great advantages to MAMMOTH is that it is natively coupled to various MOOSE-based multi-physics codes. For this exercise, MAMMOTH is to be used in 3-D, time dependent, diffusion mode.

There are two main approaches. The first is to use a Monte Carlo calculation to determine quantities of interest at various state points and then interpolate between these values based on the results of the point kinetics models. The second method is to develop homogenized cross sections from a transport code at various state points which are then used in MAMMOTH for 3-D, time dependent diffusion calculations. The state points are changes to the core or sample state. Some of the changes are reflected in average core temperature, control rod positions, and temperature in the experiment.

The methodology for each calculation approach is illustrated below in Figure 2 along with a more detailed description for each path.

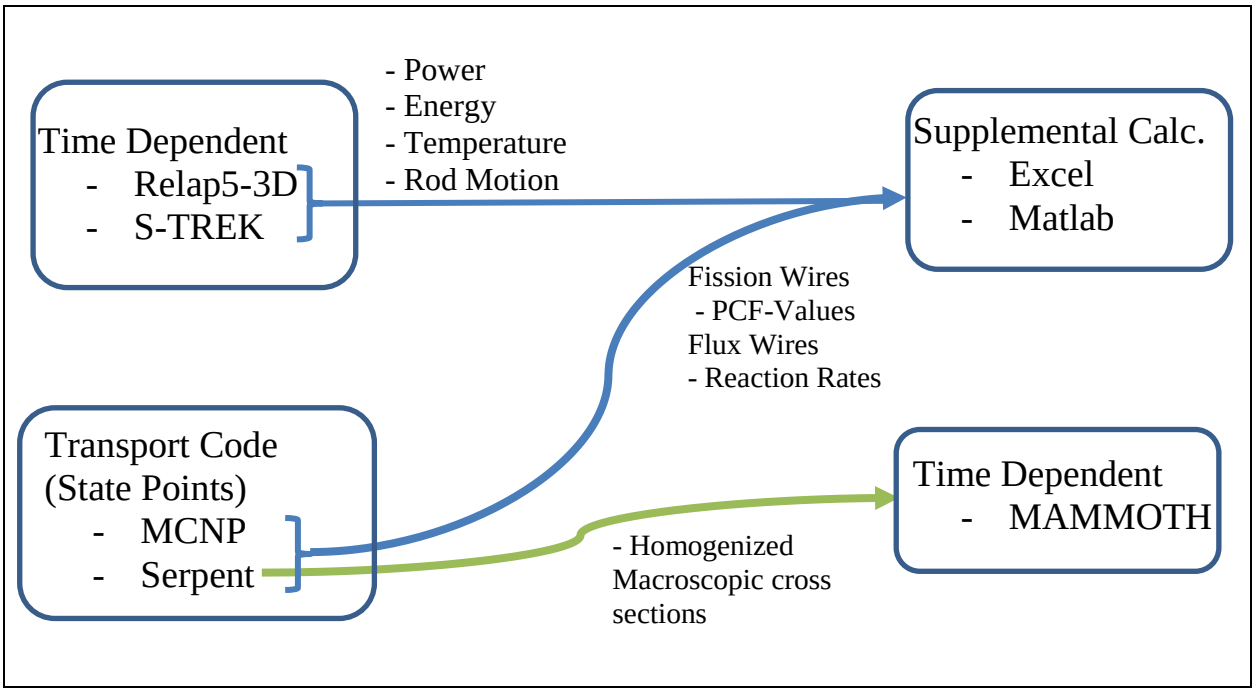

Figure 2. Modeling Pathways.

3.2.1 RELAP5-3D and S-TREK

RELAP5-3D has a built-in point kinetics solver and can perform several other simple supplemental calculations as needed. RELAP5-3D has many more abilities than point kinetics, but that is the primary feature used here. S-TREK is a point kinetics solver that was built for TREAT and meant to duplicate the code from the automatic reactor control system (ARCS) at TREAT. Supplemental calculations are performed for both RELAP5-3D and S-TREK as needed. RELAP5-3D and S-TREK provide reactor power, control rod position, and energy vs. time data. Supplemental calculations are required to convert energy to temperature for S-TREK while RELAP5-3D calculates it internally. In both cases, the same correlation from energy to temperature and rod worth curves were used to maintain uniformity. In other words, both codes should generate similar results given the same input.

The first step in the calculation process is to develop a set of PCF and reaction rates for specific state points. The state points are determined by the variables that may influence the PCF or reaction rates. It was determined that the three variables to investigate would be average core temperature, control rod position, and wire temperature. By calculating state points, 3-D transport information can be transferred to the 0-D time dependent point kinetics model. Additionally, it has been shown that the neutron detector's response is also dependent on core temperature and control rod positions [12], meaning that the reported energy/power from the neutron detectors could be biased based on the reactor state, and corrections might be needed in order to match calculation with experimental measurement.

With a matrix of state points for the PCF and reaction rates, it is possible to take the control rod position and temperature and linearly interpolate the instantaneous value for the PCF or reaction rate. The integration of the instantaneous PCF value or reaction rate will produce the integral fissions or reactions experienced by the fission or flux wire. These integral quantities are the physical quantities that are measured after an irradiation or transient. The effective PCF or reaction rates can also be calculated from the integral quantities by dividing by the energy put into the reactor. For a simulation, the energy is a direct quantity obtained by the calculation, but, for the real experiment, it is inferred from neutron chambers that have their own variations and biases.

3.2.2 MAMMOTH

MAMMOTH is to be used to perform 3-D neutronics calculations using diffusion. However, MAMMOTH requires a set of homogenized macroscopic cross sections. Just like the RELAP5-3D and S-TREK calculation paths for the PCF values, MAMMOTH relies on several Monte Carlo calculations but uses the calculations for a different purpose. Serpent is used to develop cross sections at each state point, and MAMMOTH performs 3-D time dependent calculations by interpolating between the cross sections. In reality, the cross section does not need to be developed from a Monte Carlo code. Deterministic codes can also be used. The advantage of MAMMOTH is that it will develop a multi-dimensional temperature profile (assumed to be flat for RELAP5-3D and S-TREK) and it takes into account other 3-D time dependent effects that are absent in by point kinetics. MAMMOTH does not rely on a rod calibration curve or a temperature feedback curve. All three codes, however, rely on thermal properties such as specific heat and thermal conductivity. Another advantage of MAMMOTH is that it can couple with other MOOSE-based codes, including the BISON [13] fuel performance application, which is important for modeling more complex experiments that require more physics and cannot be covered by point kinetics.

3.3 Assumptions/Approximations

As hinted in the prior section, all Monte Carlo calculations use a flat temperature profile. In reality, there is a temperature profile that starts flat at the beginning of a transient or an irradiation. As more energy is added to the core, the temperature distribution is built up. Due to the time scale difference in transient or irradiation mode, we can expect the distribution to be different. For a transient, it is a good approximation to assume that the system is adiabatic (no heat removal) from the core. However, during the LLSS irradiation, there is ~2 hours for the heat to exit, and the temperature profile is expected to be different than a transient.

In an effort to not over complicate the issue for an analysis, it was decided that it might be a fairly good argument to suggest that the average core temperature would be sufficient to characterize the PCF and reaction rates. The validity of this argument has not been proven. But, nevertheless, the analysis will use the assumption. The assumption of a flat temperature profile is more important for RELAP5-3D and S-TREK. The only implication for MAMMOTH is that the cross sections were developed with neighbors near it using the same temperature. This assumption depends on the gradient of the temperature and the cross sections' reliance on its neighbors. In other words, RELAP5-3D and S-TREK are making a bigger assumption, while MAMMOTH is making a much smaller assumption.

RELAP5-3D and S-TREK rely on supplemental data sources to describe the power feedback due to temperature and the heat required to raise the temperature (thermodynamic properties). The value and usage of these data are only as good as their applicability and contain inherent uncertainties from their creation. For instance, the M8 core has 2 power feedback tables (half-slotted and full slotted), and there is an additional (more conservative) table in the TREAT Safety Analysis Report (SAR).

RELAP5-3D and S-TREK rely on rod calibrations that are measured, while MAMMOTH relies on the cross sections. The issue with a rod calibration is that the worth of control rods are relative to the rest of the core. Given the enormous magnitude of the worth of the transient and control shutdown rods, it is likely that substantially different results could be obtained for the same rod movements if the rest of the rods in the core are at different configurations. The argument here gets back to the basic premise that reactivity is an integral term. Section 4.1.1 gives an example of how the measured reactivity for a transient differed from the rod calibration curve. However, Section 5.1.3 showed that an independent analysis of the differential rod calibration data produced a different rod calibration curve that matched closer to the measured reactivity for the transient. A full assessment of this issue has not been evaluated for the sensitivities, but it appears to be less than 0.07 %Δk/k (10 cents).

Additional assumptions get back to the main assumptions used with the codes themselves and the developed models. For instance, MCNP and Serpent rely on cross sections that have uncertainties and covariances in the microscopic cross sections that are not propagated through to the end result. The uncertainties reported are statistical results associated with the number of particles in a run but not the underlining physics. Additionally, there are uncertainties in the models, since one developer may make a model different than what exists in reality in both geometry and isotope concentrations. For the point kinetics models, there are assumptions of time and flux shape independence, which is clearly violated but has proven through history to be very good. There are numerous other assumptions and simplifications that exist for this analysis of which the analysts may have no knowledge of their existence or applicability. Further, measured values used for inputs in calculations have uncertainties and biases. In no practical way is anyone able to model perfectly what actually exists. Instead, the best engineering judgment is used to identify the most significant variables along with available tools that can achieve a result in a practical manner.

In no way can one assume that the results of this exercise will be sufficient to inform all future modeling of the PCF. The modeling requirements may change with required physics, modeling tools available, and ability to achieve solutions in a reasonable time and budget. However, the results presented here are a good first step.

4. ATF-3 TRANSIENT PRESCRIPTION TESTS, MODELING ANALYSIS

Below are detailed various questions that were explored to help gauge the required variables for modeling the LLSS, 1.5% natural transient, and 2.6% clipped transient. In particular, it is advantageous to cut down on the number of required state points since one Monte Carlo calculation can take a day or two (i.e., one state point). These studies were performed assuming a 0.36 wt% depleted uranium wire, but the behavior is not expected to change for the 0.2 wt% enrichment.

4.1 Temperature and Control Rod Dependence

It is well known that the temperature and control rods can influence the PCF value. [12] The PCF value at the various states can give an indication of the dependence on each of these variables. The states for the control rod position and temperature could be estimated using the assumed rod positions vs. time and temperature vs. time data from RELAP5-3D and S-TREK. However, RELAP5-3D and S-TREK are used with transient rod calibration curves and assume the reactor is in a critical configuration with all the other control rods at the beginning of the calculation. The position of the control/shutdown rods that would make the core critical had to be estimated using a Monte Carlo code with the transient rods in their pre-defined cocked position before the transient. The temperature from point kinetics is derived from the integration of the power (i.e., Energy) over time, using some thermodynamic properties and the mass of the core. The entire process is assumed to be adiabatic. Back of the hand calculations have been performed and have shown that thermal conductivity for TREAT's graphite does not matter for time scales on the order of 1 minute. Sensitivity calculations with simple and detailed RELAP5-3D models [14] also confirm that the thermal conductivity of the graphite does not matter for time scales on the order of 1 minute.

For the LLSS irradiation, the control rods and temperature are directly related since the operators move the control rods manually to adjust for the power decrease caused by temperature. A model was created from recorded temperature data of the last heat balance to estimate the rod and temperature change during the irradiation. Each of the thermocouple data was fit to an equation $T(t) = (T_{asy} - T_0)*(1-\exp(-st)) + T_0$. Where T_0 is the initial temperature, T_{asy} is the asymptotic temperature and s is the time constant to reach saturation. The time constant was taken as an average over all of the thermocouples and was found to be 1.046/hour. The control rods and average temperature could be estimated for each step during the 2 hour run, assuming the time constant applied to both quantities. The control/shutdown rods were expected to move from 21.7 inches to 26.9 inches, and the temperature was expected to go from 294K to 357K. The PCF values were obtained for both the beginning and ending states.

In the 1.5% $\Delta k/k$ natural shaped transient, the transient rods move from ~27.9 inches to 40 inches. The transient rods are fully ejected before the reactor gains much power (~1MW). For the case of a natural shaped transient, the rod movement variable can safely be eliminated by assuming that the rods are in the fully withdrawn position (40 inch). This is a useful result for later studies since the core is limited to one variable instead of two. Further, the dependence of the core on temperature can be isolated. ECAR-3907 has provided a useful table to aid in prediction of PCFs as long as the PCF can be described as a polynomial as a function of average core temperature. Figure 3 shows the Serpent calculation of the PCF values versus average core temperature, and Figure 4 shows the center position isolated to show the linear dependence. Refer to Figure 1 for placement of the positions.

The results show a clear linear trend and a large change based on axial position, which was expected since the fission wires are exposed to lower fluxes due to the increased thickness of the Dy filter and distance. In every case, the PCF changes by ~11-13% as the core heats up.

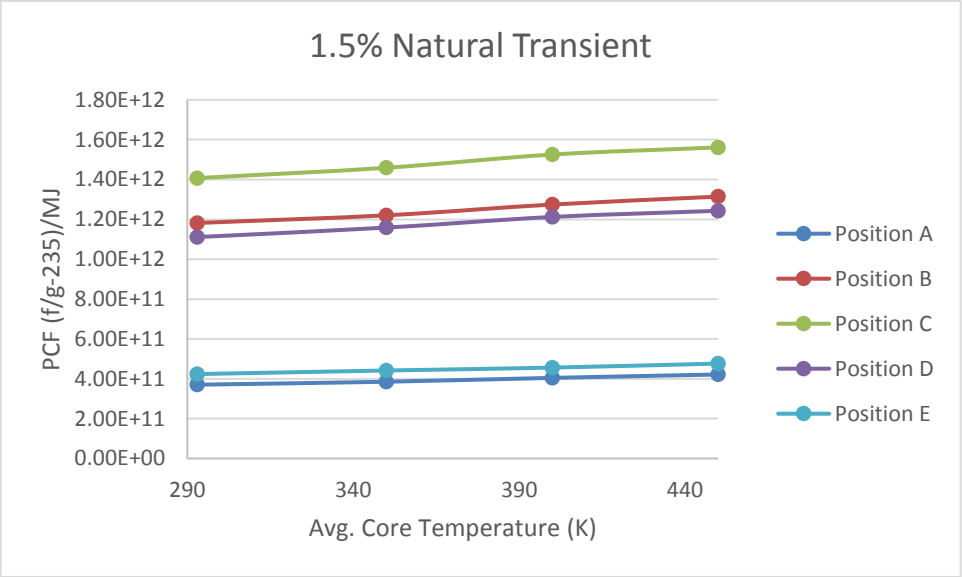

Figure 3. PCF Temperature dependence for Core Temperature.

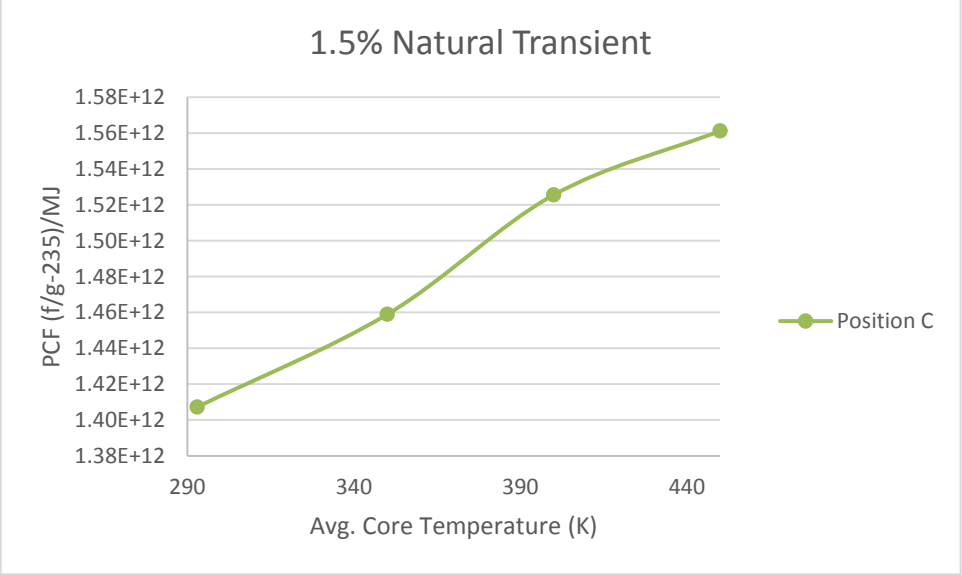

Figure 4. Center PCF Dependence on Temperature for the 1.5% Natural Transient.

The clipped 2.6% Δk/k transient is the most complex and requires the consideration of the control rods. In order to get an estimate of the state dependence, S-TREK and RELAP5-3D data were used to plot the transient rods position vs. the average core temperature, and the S-TREK data are shown below in Figure 5. The RELAP5-3D and S-TREK data are nearly identical.

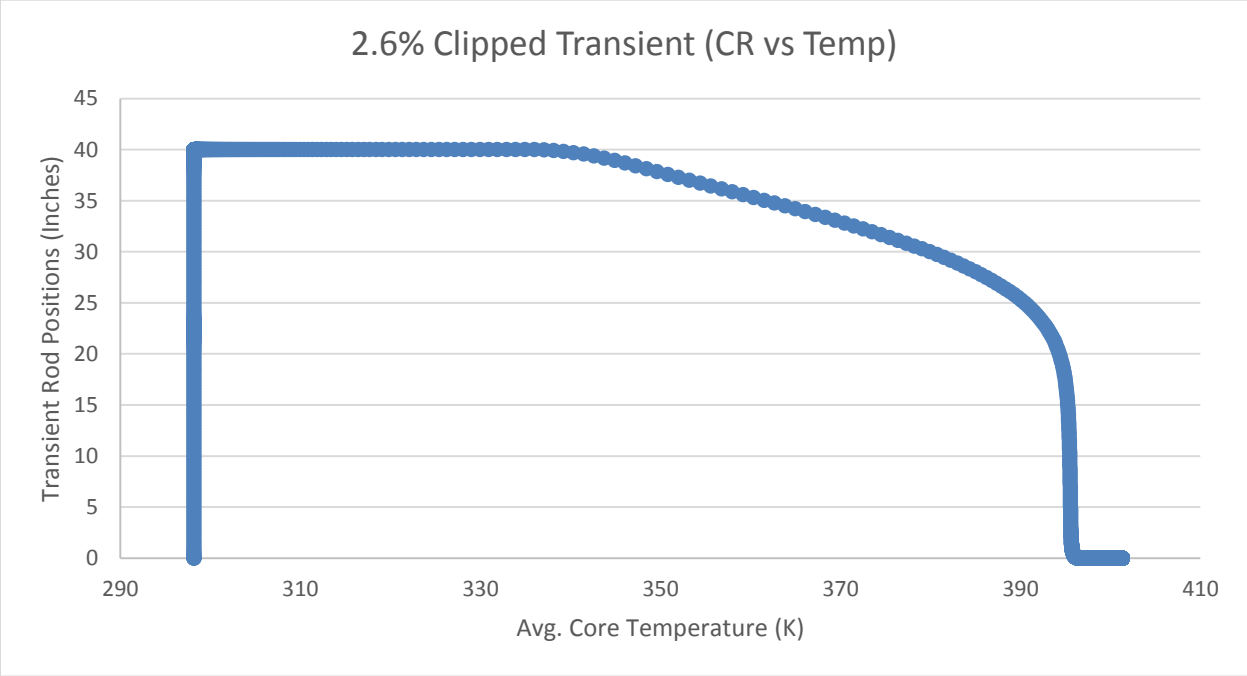

Figure 5. Control Rod vs Temperature for the 2.6% Clipped Transient.

From the chosen state points for the 2.6% clipped transient, a 3-D plot was generated to show the PCF dependence on control rods and core temperature. Figure 6 shows the result for sample Position C. Two fits are presented. One uses all the data, and the other ignores the data with the transient rod at 0 inches since there is an obvious non-linearity, and the control rods in the 0 inch position do not contribute much to the 2.6% clipped transient. However, even with a different fit, this results in a change of less than 1.8% for all axial positions, with the worst being at position A. Even with the data being slightly non-linear, a linear assumption works fairly well.

The fit with the data towards the 40 inches is considered the more applicable fit since the later data are more important in the transient. Overall, the dependence on the control rods is just as large if not larger than the core temperature dependence. For all axial locations, the percentage change due to control rod movement from 0 to 40 inches for a specified temperature cause the PCF to change by ~14-23%. Note, that the units are per U-235 gram, not the wire. If dividing by the mass of the wire, the slope of the plane is lessened.

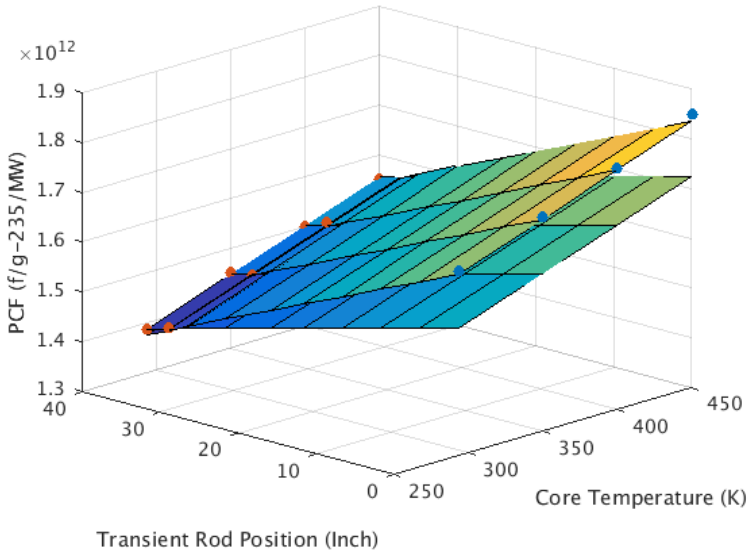

Figure 6. PCF Dependence on Control Rod Position and Core Temperature for Sample Position C.

Table 4 shows the chosen state points for the three reactor runs, taking into account the core temperature and control rod positions.

Table 4. States Points for Each of the Reactor Runs.

Reactor Run	State #	Control Rods (Inch)			Avg Core Temperature (K)
		C/S	Transient	Compensation	
LLSS	1	21.7	40	Fully Out	294
	2	26.9	40	Fully Out	357
1.5% Natural	1	27.1	40	Fully Out	294
	2	27.1	40	Fully Out	350
	3	27.1	40	Fully Out	400
	4	27.1	40	Fully Out	450
2.6% Clipped	1	30.5	0	Fully Out	294
	2	30.5	0	Fully Out	350
	3	30.5	0	Fully Out	400
	4	30.5	0	Fully Out	450
	5	30.5	24.1	Fully Out	350
	6	30.5	24.1	Fully Out	400
	7	30.5	37.3	Fully Out	300
	8	30.5	37.3	Fully Out	350
	9	30.5	37.3	Fully Out	400
	10	30.5	40	Fully Out	294
	11	30.5	40	Fully Out	350
	12	30.5	40	Fully Out	400
	13	30.5	40	Fully Out	450

4.1.1 Application of Temperature and Control Rod Variables to M8 Data

A simple deviation was taken at this point to develop a 3-D graph of PCF as a function of temperature and control rod position for old M8 calibration data to compare against and to determine if these two variables would be sufficient to quantify the PCF value. The power history and energy versus time data was available for many transients and could take the place of RELAP5-3D or S-TREK. Additionally, the measured total fissions and energy from the core were also available. However, it was found very quickly from the first transient analyzed (T2873) that the final PCF value changed greatly depending on which chamber history was used. It appeared that the best agreement came from a logarithmic channel. Figure 7 below shows the power history differences between one of the linear and logarithmic channels for the 2873 transient.

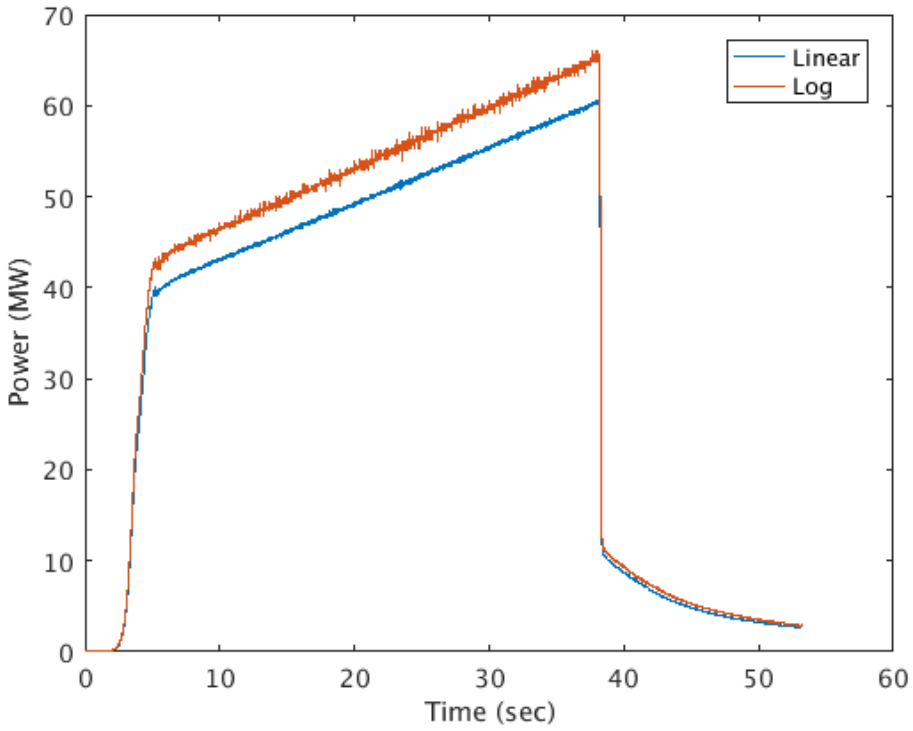

Figure 7. Linear and Logarithmic Profiles for Transient 2873.

More data sets were analyzed primarily from the M8CAL series, and the core energy was calculated using the linear, log, and energy channels. There was a clear spread of 22-59% in old data, while the more recent data since TREAT's restart varies from 13-24%. The energy channels by themselves varied much less ~1 to 14% for both historical and present data. The variation in all of the channels seemed to have a clear connection with the shape of the transient. There is no reason to say that one chamber should be considered more correct than another besides the naming scheme, especially since the energy channels are linear channels with the only difference being the integration of the charge. Figure 8 below shows a clear increase in variation in the energy calculated from each chamber for transients 2886-2888 which are since the restart of TREAT. Transients 2886-2888 were ~1.8%, ~3.15% and ~4% Δk/k step changes in reactivity, respectively. Because of the large variation, there is no benefit to substituting the chamber history for RELAP5-3D or S-TREK histories, and the energy channels' readings are suspect in their applicability to report the "true" energy value.

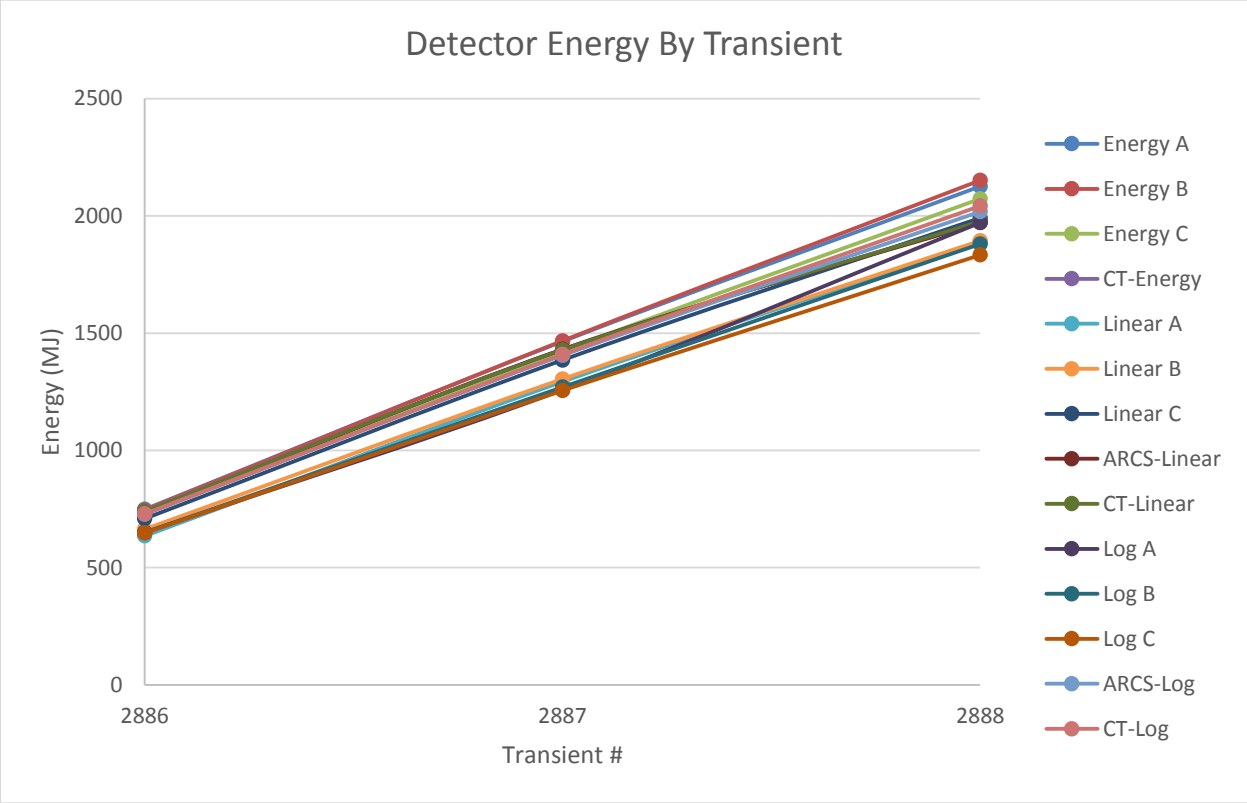

Figure 8. Energy Variation for Transients 2886-2888, Post-Restart.

Further, when a transient is performed, it is impossible to specify the exact amount of reactivity as required. While the variation in the process is unknown, ball park estimates place it at ~0.07% Δk/k. There could be several reasons for the variation such as bias in the calibration data or repeatability of the control system. Some work has been done to determine how much bias is in the calibration data. Data were plotted from the reactivity computer of the reactivity vs. position for transients 2886 and 2888. These two graphs were plotted with the control rod calibration curve using the present methods for rod calibration. The graphs had to be shifted in the y-axis for overlap due to the starting point always being 0. It is believed the initial curve was due to some of the rods being delayed in the transient. Figure 9 shows a clear under-prediction by the rod calibration method. This is not surprising since reactivity is an integral value, which means that the reactivity value depends on the configuration of everything in the core. The rods in a transient situation are substantially different than during rod calibrations where the reactor is kept near critical.

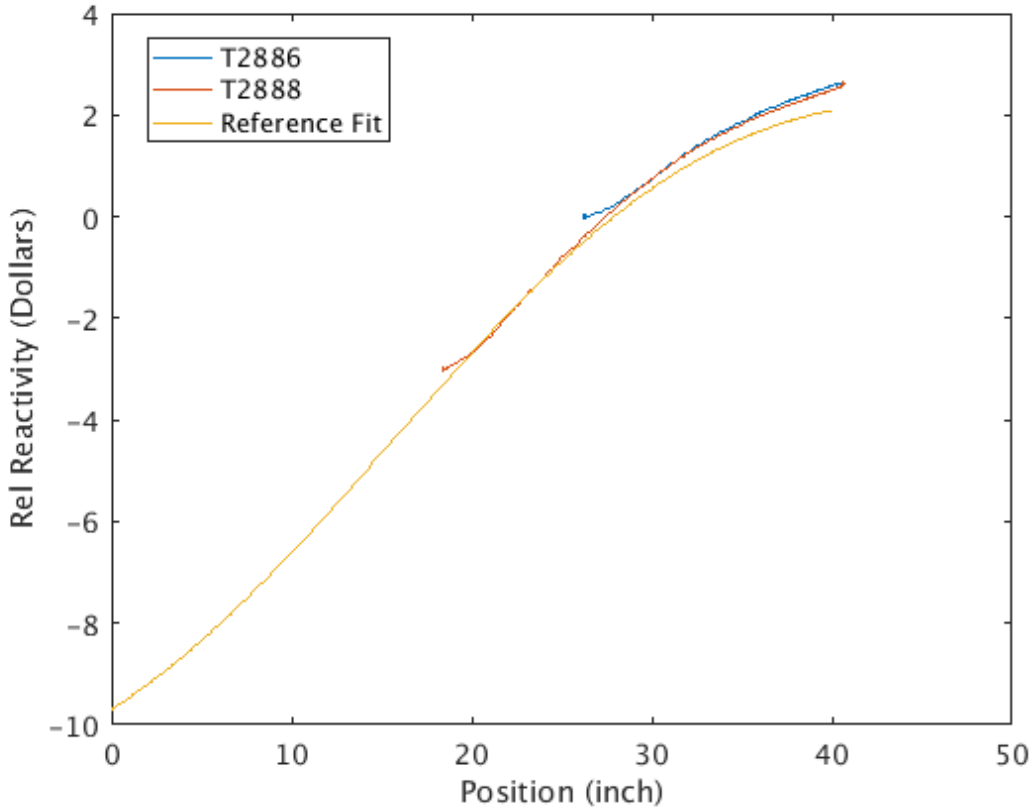

Figure 9. Measured Transient Rod Worth Curves from Transients and Compared to the Rod Calibration Curve.

These results present a very interesting predicament. One would like to use a measured power history to revise results since a modeled situation is ideal and does not take into account other sources of variation. However, given the large spread in data, it is recommended to calculate the total fissions per gram for a sample using the modeled power history (for a specified reactivity) and then compare it with the measured total fissions per gram. The modeled power history could be modified by changing the reactivity to what actually was measured to obtain a more precise answer. After comparing the modeled and measured total fissions per gram, adjustments can be made to potentially determine a best estimate of the total energy in the core. Other comparisons and analysis might be possible as well. The end result is that the chamber energy readings have a rather large uncertainty and cannot be taken as a well known term when comparing modeled data with experimental data.

4.2 Sample Temperature Dependence

In an effort to determine how much the PCF depends on the change in temperature of the sample, a set of PCF values was calculated by varying core temperature and the Uranium temperature. Table 5 shows the Serpent results in units of f/g-235/MW and the difference between the largest and smallest values. The values came from the control/shutdown rods placed in a prototypic location of a 2% Δk/k natural transient and the 0.36 wt% enrichment. This calculation was done before the 1.5% natural transient was defined as the instrumented transient. Nevertheless, the results show that there is less than a 2% change in the PCF due to temperature over an 1100 degree change, which is fairly insignificant. That magnitude of uncertainty is probably within the limits of the model itself or the PCF result accuracy. The temperature of the sample can be safely ignored. However, it is possible to specify a sample temperature

that is in the neighborhood to reduce the error and eliminate a dimension to the variable matrix for state points. Further, if one is looking for a conservative estimate, the room temperature seems to be a good choice. The state points were calculated by specifying a sample temperature that was reasonable to within a few hundred degrees.

Table 5. PCF Dependence on Sample Temperature.

Core Temperature (K)	Sample Temperature (K)					1400K to 294K % Difference
—	294	600	800	1000	1400	—
294	1.48E+12	—	—	—	1.50E+12	1.4
350	1.56E+12	—	—	—	1.55E+12	-0.7
400	1.63E+12	1.61E+12	1.61E+12	1.60E+12	1.60E+12	-1.8
450	1.66E+12	—	—	—	1.64E+12	-1.0

4.3 Detector Bias

Neutron detectors are the means of specifying the power level in TREAT, and, as such, it may be important to quantify how well the reading represents the true phenomena. In a water reactor, power quantification is not too difficult. However, TREAT has an open loop system and uses air as its coolant.

The process of calibrating TREAT neutron detectors is performed in the following manner. First, the reactor is brought up to ~80kW and held there until the rods do not need to be modified for quite some time. The flow rate and change in temperature are used to estimate the "true" power level. Second, the chambers are then moved closer or further away from the core, so that the voltage output of the chamber is near a specified value. Each of these steps has an unknown amount of bias and uncertainty associated with it. The precision (meaning how close the values are to each other) of the results can easily be identified to be ~20% for transients. The actual bias (meaning how far off from the true value) is unknown, and the actual uncertainty in a value is unknown.

Ignoring all the issues associated with how TREAT detectors are calibrated, there is another issue. When neutron detectors are calibrated, it is assumed that the number of neutrons the detector is observing is proportional to the power, and the calibration defines the proportionality constant. However, when there are drastic temperature and flux shape changes, the proportionality constant also changes. The magnitude of the change depends on several factors such as distance from the core and filters surrounding the chamber. It has been shown that steady state chambers can report changes of 30% in power. The transient chambers have much less of a bias than the steady state chambers. [12]

In order to estimate the bias in the chambers for the LLSS, 1.6% natural transient and 2.6% clipped transient, calculations are performed to estimate a relative B-10 reaction in the detector holes. The reactions must be normalized to the prototypic conditions of the reactor during the heat balance in order to estimate how far off the chamber will read. Just like PCF values, the bias to the detector can be calculated for each state point and applied to indicate what the measured power would be (ignoring all other biases and uncertainties except the proportionality constant) for comparison with simulated data.

Several calculations were performed to obtain relative detector responses for the states involved in the 2.6% clipped transient and are shown in Figure 10.

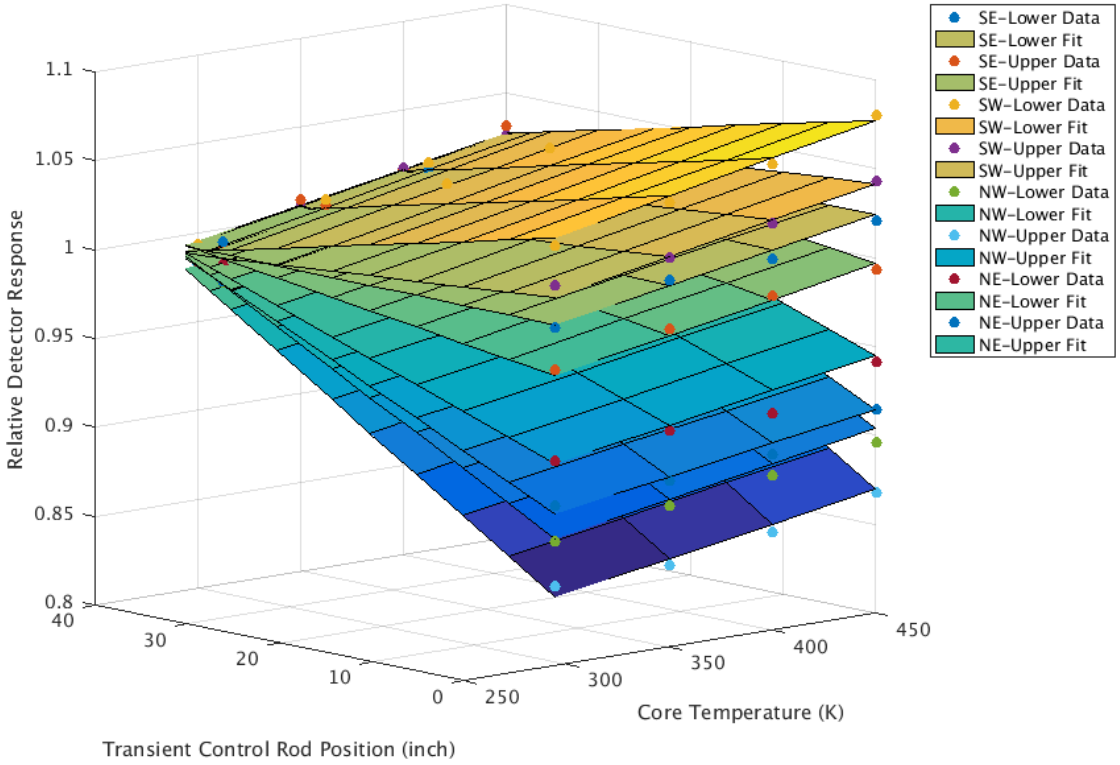

Figure 10. Relative Transient Detector Response.

While the relative detector responses varied by up to ~16%, when they are applied to the 2.6% clipped transient, the detector response for predicted energy would be less than 4% different than the true value as seen in Table 6. This shows that the observed change of ~22-59% in energy for all detector types is not largely due to the proportionality constant changing from control rod position or temperature. The more likely cause of the spread in the detector data is probably due to the heat balance method of detector adjustment and calibration settings. The uncertainty in the heat balance does not influence the spread in detector readings.

Table 6. Detector Proportionality Constant Bias for 2.6% Clipped Transient.

Detector Energy (MJ) Ref = 586.7 MJ	% Different	Detectors	Location
592	0.90	Log-C	SE-Lower Hole
586.1	-0.10	Linear-C, Energy-C	SE-Upper Hole
597	1.76	Log-B	SW-Lower Hole
588.6	0.32	Linear-B, Energy-B	SW-Upper Hole
579.2	-1.28	Log-A	NW-Lower Hole
568.3	-3.14	Linear-A, Energy-A	NW-Upper Hole
583.7	-0.51	Nothing	NE-Lower Hole
575.8	-1.85	ARCS-Log, ARCS-Linear	NE-Upper Hole

The relative detector response can sometimes be much more important for steady state mode, depending on how far different the state of the core is from the state in which the core was at during the heat balance. A Serpent calculation was performed that estimated the detector bias for the two state points in the LLSS, and the worst result was 1.2% different. The calculation was operating under the assumption that the LLSS irradiation would be performed by banking the control/shutdown rods while leaving the transient rods fully withdrawn and then slowly removing the control/shutdown rods to compensate for temperature. The compensation rods are always assumed to be removed. This type of configuration is very similar to the heat balance, and it is no surprise that the detector response would be very close. However, if the transient rods are inserted, a much different result would be expected.

The relative response for the 1.5% natural transient can be inferred by looking to Figure 6 and noting that the rods are at 40 inches for the whole transient. The expected results would be less than 5% and can be safely ignored. While Figure 6 was developed for a fixed control/shutdown rod position, that difference is a movement of 3 inches, which would not be expected to change the results drastically.

4.4 Inter-model Comparisons

The results between RELAP5-3D and S-TREK showed very little difference. This was expected, since the temperature feedback table and control rod worth curves were kept consistent.

The difference between the model used in MCNP and the one used in Serpent did show significant differences in the PCF values with changes in the transient rod's position and a slight change with temperature. Figure 11-Figure 12 below show the difference in the PCF values for the 2.6% clipped transient with the transient rods at 0 and 40 inches.

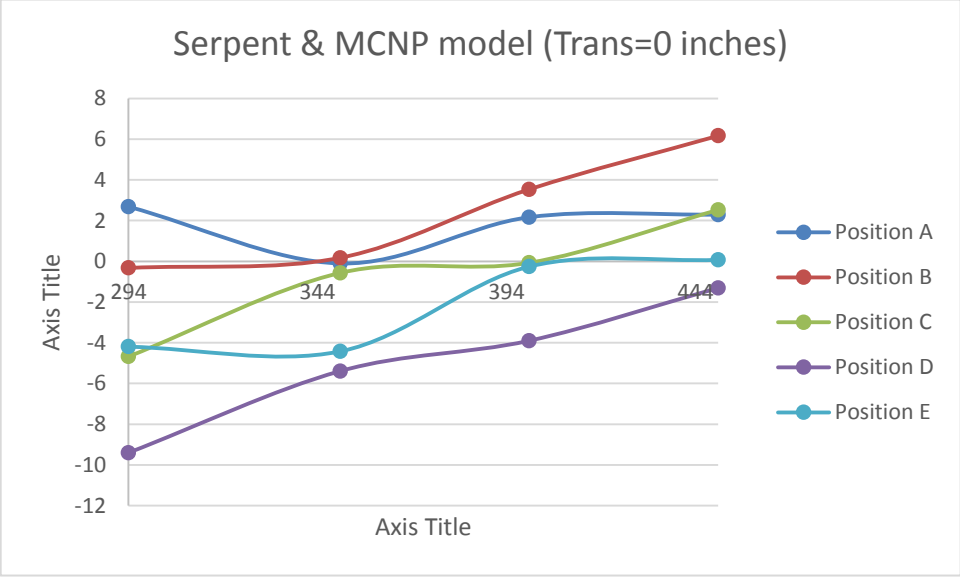

Figure 11. Difference in PCF's with Transient Rods at 0 inches for the 2.6% Clipped Transient.

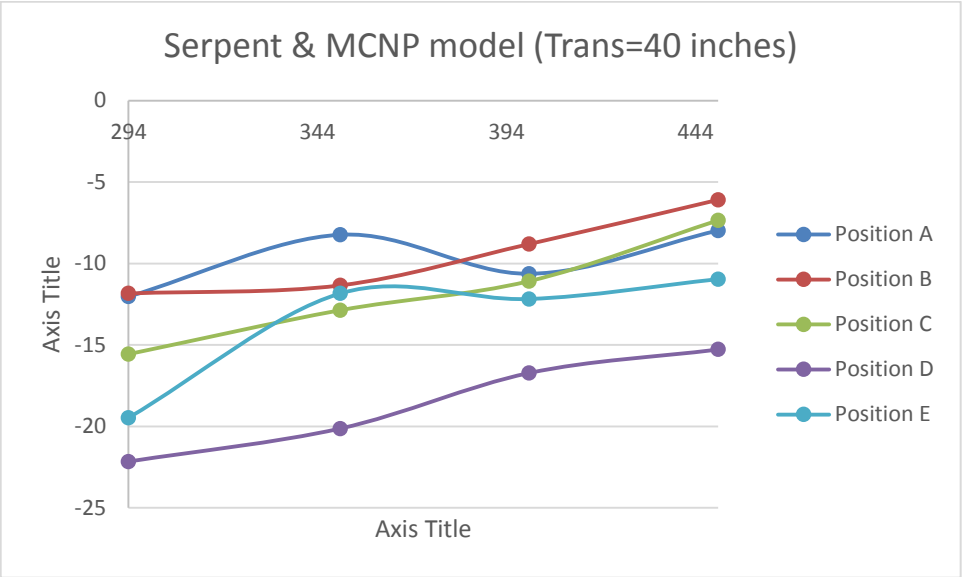

Figure 12. Difference in PCF's with Transient Rods at 40 inches for the 2.6% Clipped Transient.

While the individual state point PCF values were different by up to ~22%, the effective PCF values are less, since the effective PCF is dependent on the state points and how long the reactor is near that state. For the 2.6% clipped transient, the difference between the PCF for the Serpent and MCNP models were all within 16%. Further, this does not mean that there is some problem between MCNP and Serpent. Instead, the differences are most likely due to differences in the model design or material compositions.

5. ATF-3 TRANSIENT PRESCRIPTION TESTS, DATA ANALYSIS STAGES

This section is dedicated to demonstrating the evolution of the modeling predictions. There are three main stages. The first stage shows calculations using data inputs that were provided from the data package and other initial estimates. These calculations are considered blind predictions since they give the best estimates before the experiment was ever performed.

The second stage makes use of as-run data to modify the predictions and provides an estimate of how much the results change between the hypothetical run and what actually happened.

The third stage considers changes that are made to modeling predictions and measurement calculations once measurements were made. Once measurements are made, there is a tendency for researchers to want to make calculations and measurement match by searching for mistakes, missing phenomena, or tuning parameters. There are several parameters and calculations in both the modeling and measurement that can be adjusted to tune predictions and measurement. These parameters are not always apparent in presented results and are representative of true uncertainties in the methods. Further, feedback between predictions and calculations can help identify missing phenomena that were not considered or blatant mistakes. The third stage tries to highlight the tunable parameters, mistakes, and understanding gained in this phase. The reader should keep in mind that there are three distinct entities of interest here. They are: modeling, measurement, and reality. There tends to be a tendency to think that measurement is reality. This is not true. Modeling and measurement have multiple tunable parameters and rely on various assumptions and built-in uncertainties in order to arrive at their final conclusions.

The final sub-section provides a review and highlights from the three stages.

5.1 Calculation Results (pre-transient)

Below are results for the DU wires for each case of the reactor runs. These results are considered pre-transient because they are the initial calculations before any knowledge has been gained about what actually happened during the runs. These calculations assumed 0.32 wt% U235 composition in the DU wires. The enrichment changed once the laboratory analysis was complete, but this occurred after the runs were already performed, and the changes are covered in Section 5.2.

5.1.1 LLSS Irradiation

The LLSS results do not depend on RELAP5-3D or S-TREK but only on a Monte Carlo code. The calculated energy for 2 hours is ~581.5 MJ, if the power history is kept constant at 80kW based on the DIS steady state linear channel. The Distributed Information System (DIS) linear channel should report ~576 MJ, which is 2 hours multiplied by 80 kW. However, due to detector bias, the core should have received 1% more energy than reported by the chamber. There may also be added energy due to the startup and unreported time by the operators, since the process of reporting is manually done, and the fission and flux wires will be influenced by the entire power history, not just when 80kW is reached.

Table 7 has the predicted results using the Serpent and MCNP models. The thing to notice is the designation of the MeV/fission for each row. For most analysis, 200 MeV/fission is assumed. However, many historical documents reference ~182 MeV/fission. This is the reason that Serpent was set to 182 MeV/fission. The MCNP model results were given from both F7 and F4 tallies. The F7 tally uses a predefined value of 180.9 MeV/fission for Uranium 235 fission. The F4 tally requires the user to provide their own estimate of the fission energy deposition. Initially, the F4 tally was being reported using 200 MeV/fission, and the results matched fairly well with the Serpent model for all results including the 1.5% and 2.6% transients. However, it does not make sense to make this comparison. While the results looked good between the two codes, it makes more sense to use a consistent fission energy deposition. The LLSS results differed between the two models by ~7 to 16%.

Table 7. LLSS (Pre-Transient) Modeling Estimate of PCF.

	Units - f/(g-U235-MJ)				
	Position A	Position B	Position C	Position D	Position E
2 Hours (Serpent Model 182 MeV/f)	3.89E+11	1.22E+12	1.46E+12	1.16E+12	4.39E+11
2 Hours (MCNP Model 180.9MeV/f)	4.18E+11	1.34E+12	1.66E+12	1.39E+12	5.04E+11
2 Hours (MCNP 200MeV/f)	3.78E+11	1.21E+12	1.50E+12	1.25E+12	4.56E+11

5.1.2 1.5%Δk/k Natural Transient

The results for the 1.5% natural transient are shown below in Table 8. RELAP5-3D produced a transient with 593.7 MJ and S-TREK had 576.4 MJ. The results for the total fissions/gram differed by ~3% between RELAP5-3D and S-TREK. This discrepancy is due to the total energy difference. RELAP5-3D and S-TREK should have the same result given the same input. The reason for the 3% difference in energy is due to the user selecting a rod position that would produce a transient close to 1.5% but not exactly. The PCF values are nearly identical between REPLAP5-3D and S-TREK, since the PCF value divides by the energy. There is a difference in the PCF values depending on the Monte Carlo model. The MCNP and Serpent models' PCF values varied from 7% to 15% in the same fashion as the LLSS results.

Table 8. 1.5% Natural Transient (Pre-Transient) Modeling Estimate of PCF.

	Units - f/(g-U235-MJ)				
	Center A	Center B	Center C	Center D	Center E
RELAP5-3D (Serpent)	3.88E+11	1.23E+12	1.47E+12	1.17E+12	4.43E+11
S-TREK (Serpent)	3.88E+11	1.23E+12	1.47E+12	1.16E+12	4.42E+11
RELAP5-3D (MCNP)	4.22E+11	1.34E+12	1.66E+12	1.38E+12	5.10E+11
S-TREK (MCNP)	4.21E+11	1.34E+12	1.66E+12	1.38E+12	5.10E+11

5.1.3 2.6%Δk/k Clipped Transient

The pre-transient results for the 2.6% clipped transient are shown below in Table 9. The fissions/gram and PCF results between RELAP5-3D and S-TREK are nearly identical for a fixed Serpent or MCNP calculation value set. The reason they are nearly identical is because the reported final energy from RELAP5-3D is 588.89 MJ and 586.7 MJ for S-TREK. The PCF changes more between the Serpent and MCNP models with differences of ~9.5 to 16%.

Table 9. 2.6% Clipped Transient (Pre-Transient) Modeling Estimate of PCF.

	f/(g-wire-MJ)				
	Position A	Position B	Position C	Position D	Position E
RELAP5-3D (Serpent)	3.82E+11	1.23E+12	1.48E+12	1.18E+12	4.53E+11
S-TREK (Serpent)	3.83E+11	1.23E+12	1.48E+12	1.18E+12	4.52E+11
RELAP5-3D (MCNP 180.9 MeV/f)	4.23E+11	1.36E+12	1.68E+12	1.40E+12	5.17E+11
S-TREK (MCNP 180.9 MeV/f)	4.23E+11	1.36E+12	1.68E+12	1.40E+12	5.17E+11

5.2 Results Using As-Run Data

This section presents results after the transient prescription runs were performed. This section makes use of reactor data collected during the runs to determine if added information from the run is useful. The data do not include the sample measurements and were performed without the knowledge of these results. While in this phase, measurements of the DU enrichment were obtained. In order to compare and contrast results with Sections 5.1 and 5.3, values were calculated with both enrichments. Further, the point kinetics histories were calculated using only RELAP5-3D, since enough proof has been provided that RELAP5-3D and S-TREK provide nearly identical results.

5.2.1 LLSS Irradiation

The power history from the DIS steady state linear detector was recorded on a chart recorder during the LLSS irradiation. Integrating the DIS linear channel gave a total energy deposition of 593.6 MJ instead of the estimated 576 MJ. The estimate for the real power was calculated to be 599.6 MJ after applying the detector bias in the DIS linear channel as described in Section 5.1.1. The difference between the predicted and "as-run" energy is 4.1%. The calculations were re-run. However, given the small percentage, the results are essentially those listed in Section 5.1.1 but increased by ~3.6 to 4%. This was done using the 0.36 wt.% enrichment. The results for the 0.2 wt.% enrichment are in Table 10 and include changes to rod positions.

The reason for the difference between the desired 576 MJ and the actual run is due to two factors. The first factor is practical limitations in operations where the operators cannot hold the reactor perfectly at a fixed power level, and the second was a small period of time when a continuous air monitor (CAM) went off just as the reactor was around 50kW and a waiting period ensued while that alarm was dealt with. A graph of the DIS linear channel can be seen in Figure 13.

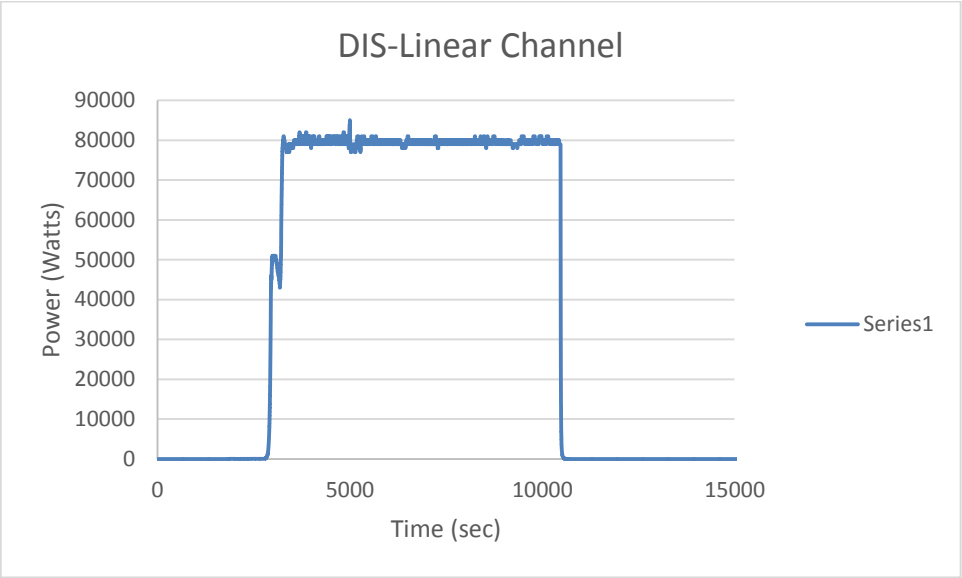

Figure 13. DIS linear channel history for the LLSS irradiation.

Recently, unofficial measurements were made in a heat balance condition to determine how different the detector value would be as compared to the last calibration. The results varied by ~ 3kW for a measurement of 80kW or 3.8%. In addition, the heat balance could have an unknown bias. It will be assumed that the DIS linear detector is correct for reactor power with the exception of detector biases explained in Section 4.3.

The reactor beginning and ending positions were noted thanks to the log sheets that had the initial rod positions written down and the reactivity computer which was turned on at the end of the irradiation and recorded the final rod positions. These positions were rather close to those initially predicted to <1 inch. Given the small inaccuracy in the rod positions, new PCFs were not calculated for the old enrichment. New PCF values were calculated using the new enrichment with the slight position adjustment. The PCF values are shown below in Table 10. The MCNP vs. Serpent models again have differences around ~8 to 12%.

Table 10. LLSS (As-Run) Modeling Estimate of PCF.

	f/g-U235-MJ				
	Position A	Position B	Position C	Position D	Position E
Serpent - As Run	4.53E+11	1.33E+12	1.57E+12	1.26E+12	5.10E+11
MCNP - As Run	4.90E+11	1.44E+12	1.77E+12	1.48E+12	5.73E+11

5.2.2 1.5%Δk/k Natural Transient

The power history from all the neutron detectors and the control rod motion was recorded during the 1.5% natural transient. It was explained in Section 4.1.1 that it would be a bad idea to use the recorded power history in place of the computed power history, since the energy of the chambers varied by ~20% when considering all chambers. The purpose of the recorded power history was to determine the reactivity, since reactivity is derived by relative shape of the power history, and the absolute magnitude does not matter. For natural transients, the timing of the control rods is of little importance since the rods are able to be fully ejected well before 1MW is reached and, thus, have little bearing on the rest of the transient since they do not move after the ejection.

The reactivity was estimated using the reactivity computer, with two log steady state chambers and several transient detectors. Reactivity was calculated using inverse kinetics. The data were used to bound the highest and lowest possible reactivity for the run. The data were 1.489% delta-k/k with a maximum of 1.504% and a minimum of 1.48%. The calculations were re-run but can be easily determined by the difference in the predicted energy and application of those percentages to those given in Section 5.1.2. Table 11 shows the energy differences. It should be pointed out that the initial calculation, while specified as 1.5%, was really somewhere between 1.50% and 1.504%. The as-run reactivity was incredibly close to the desired 1.5%. Again, this was for the 0.32 wt % enrichment.

Table 11. Energy difference between initial calculation and as run reactivity bounds using RELAP5-3D.

	Calc. Energy (MJ)	% Different
Initial	593.66	REFERENCE
1.48%	583.40	-1.76
1.50%	588.88	-0.81
1.504%	595.70	0.34

In addition, the reactivity computer recorded the power history before the transient and calculated that 7.02 MJ of energy was added before the transient occurred. This energy should be added to computed energies that only consider the transient.

New PCF values were calculated using the 0.2 wt% enrichment and are presented below in Table 12 for the 1.5% transient at 588.88MJ with an added 7.02 MJ (595.9 MJ). Adjustments were also made to positions of the control shutdown rods since the as-run positions were 0.5 inches different than assumed for the initial analysis. Calculations were performed using RELAP5-3D. The result is independent of using RELAP5-3D or S-TREK.

Table 12. 1.5% (As-Run) Modeling Estimate of PCF.

	fissions/(g-U235-MJ)				
	Position A	Position B	Position C	Position D	Position E
Serpent (595.9 MJ)	4.50E+11	1.32E+12	1.57E+12	1.27E+12	5.15E+11
MCNP (595.9 MJ)	4.80E+11	1.44E+12	1.75E+12	1.46E+12	5.81E+11

5.2.3 2.6%Δk/k Clipped Transient

Like the 1.5% natural transient, data for position and power history were recorded for the 2.6% clipped transient. Unlike, the 1.5% natural transient, not only is the initial reactivity important, but timing of when the rods move is also important. Additionally, three 2.6% clipped transients were performed. The first two demonstrated the repeatability of the transient, and the third, T2893, had the fission wires while the first two were empty.

Analysis of the three 2.6% clipped transients showed that the three runs were very comparable on all of the data available. The following quantities were compared: average reactivity, energy detector readings, travel time for each rod to move out of the core, travel time for each rod to move back in the core, and wait time between the movement of a rod. These results are presented in Table 13-Table 15. The data showed that the transient rods moved faster than expected back into the core. The maximum velocity out of the core was around 138 inches per second while the insertion was about 158 inches per second. The movement of all the rods was clearly not uniform among each of the rod drives, but each of the movements were very repeatable. The non-uniform start/stop and speedup/slowdown movement of the transient rods is shown in Figure 14. Despite the non-uniformity of the rod movements, the consistency of when the rods moved and when the rods arrived at the new positions was very repeatable.

Table 13. 2.6% Reactivity Repeatability.

Reactivity Measurement (%Δk/k)		
T2891	T2892	T2893
Avg	Avg	Avg
2.613	2.613	2.615
Max	Max	Max
2.629	2.631	2.630
Min	Min	Min
2.596	2.596	2.595

Table 14. 2.6% Energy Channel Repeatability.

	T2891	T2892	T2893
Energy A (MJ)	619.5	617.4	618.6
Energy B (MJ)	616.8	616.6	618
Energy C (MJ)	601.3	600.7	605.4

Table 15. Rod Movement Times.

Rod	Trans-1		Trans-2		Trans-3		Trans-4	
	Avg	Std	Avg	Std	Avg	Std	Avg	Std
Time Going up (sec)	0.16	1.53E-03	0.14	4.58E-03	0.18	3.61E-03	0.15	5.51E-03
Time Going Down (sec)	0.29	3.00E-03	0.30	2.52E-03	0.29	5.77E-04	0.29	2.00E-03
Start Going Up (sec)	2.01	1.15E-03	2.01	9.29E-04	2.01	2.52E-04	2.01	3.61E-04
Start Going Down (sec)	2.93	1.78E-03	2.94	1.39E-03	2.93	1.12E-03	2.96	9.29E-04

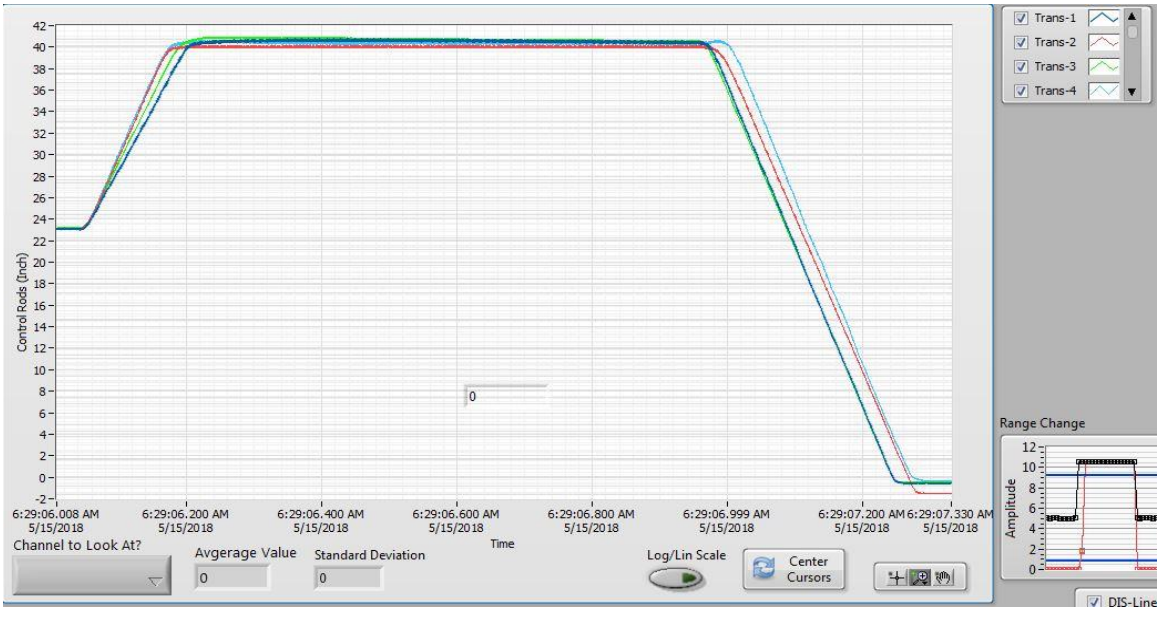

Figure 14. Transient 2893 Rod Motion.

Various sensitivity studies were performed to determine if the various artifacts of the 2.6% history would matter.

The first approach was to average all four transient rod positions for one effective rod position and decimate the data by taking 1 in 30 data points. The second approach was to try and match the initial reactivity by adjusting the initial rod position and then using the rod motion to establish timing, again with an average rod movement. For both of these cases, the control rods were not allowed to go over 40 inches, which is considered the rods full motion. However, the data clearly show that the rod did move slightly over 40 inches.

The next set of studies involved extending the available movement of the rods beyond 40 inches by extending the integral rod calibration curve. Since, the rod drives clearly have different positions, it was desired to model the individual rod movements. However, in order to do this, different rod calibration curves were needed. The raw measurement data from the differential rod worth data were obtained, and 4 rod worth curves were produced.

The third case used the original rod worth curve but extended the rod movement beyond 40 inches. The transient rods are presumed to move up to 40 inches, but given their hydraulic nature, they can move above or below when commanded to move to 40 inches. The fourth case used an average rod position using the new rod worth fit curves to maintain a true comparison with the last two cases. The fifth case used a weighted average for the rod movement by averaging the position of all the rods and weighting it by the total worth of each rod. The sixth case let each rod move independently. Table 16-Table 17 show the results from each of the cases.

Table 16. 2.6% As Run Parametric Study I.

Case	Initial position (inches)	Reactivity insertion (%Δk/k)	Clipping time (s)	Maximum power (MW)	Energy deposition (MJ)	Average fuel temperature (°C)	Maximum fuel temperature (°C)
Pretest	23.0928	2.6	0.922	3485	588.9	127.8	194.3
Posttest 1	23.0626	2.627	0.925	3635	621.0	132.4	201.9
Posttest 2	23.1146	2.614	0.925	3526	597.3	129.0	196.3

Table 17. 2.6% As Run Parametric Study II.

Case	Fit	Rod movement	Reactivity insertion (%Δk/k)	Maximum power (MW)	Energy deposition (MJ)	Average fuel temperature (°C)	Maximum fuel temperature (°C)
Posttest 3	1	Average	2.6275	3733	644.7	135.8	207.5
Posttest 4	2	Average	2.617	3684	635.9	134.5	205.4
Posttest 5	2	Weighted average	2.6156	3669	631.5	133.9	204.4
Posttest 6	2	Individual	2.6167	3663	628.4	133.5	203.7

The first set of parametric studies showed that the measured reactivity, reactivity based on control rod position, and the initial estimate, were all within 5.5%. The difference between all of these results could be considered equivalent since the rod signals had typical standard deviations of at least 0.04 inches in the signal. In other words, modeling will not produce any results better than 5% for this transient if the bounds are set by a deviation in position of 0.04 inches. However, even though the rods fluctuated at the beginning of the run by 0.04 inches, the spread in the energy channels data seems to indicate that the uncertainty from run to run is much less than 5%, in which case, it is safer to say that modeling reactivity versus the measured position could be more accurate.

The second set of parametric studies revealed that the energy increased by ~8% for Posttest 3 which should have remained nearly identical to Posttest 2. The reason for the change was due to allowing the control rods to extend beyond 40 inches. The result did not modify the reactivity by much, but it did influence the timing, since the rods had to move a little more distance which caused a little more energy deposition. This extra energy deposition is noticed throughout Posttests 4-6. Posttest 4 used the new set of rod calibration curves with a slightly different worth for the movement, putting it much closer to the measured 2.61% reactivity value. Posttests 5 and 6 indicated almost no change except for a slight energy decrease between taking an average, weighted average and individual rods. Posttest 6 is considered the most correct since it included the added physics and will be used for the RELAP5-3D power history.

In addition to the power history provided by RELAP5-3D, transient 2893 was estimated to have produced 4.9 MJ of energy before the transient occurred and should have increased the fissions in the sample by ~0.8%. The as-run control/shutdown rods were different by 1 inch, which causes a few percent difference. The PCF values given are also for the 0.2 wt% enrichment. The PCF values were calculated using the RELAP5-3D power history, and the results are shown below in Table 18.

Table 18. 2.6% (As-Run) Modeling Estimate of PCF.

	fissions/(g-U235 MJ)				
	Position A	Position B	Position C	Position D	Position E
Serpent (633.3MJ)	4.45E+11	1.33E+12	1.58E+12	1.28E+12	5.25E+11
MCNP (633.3 MJ)	4.81E+11	1.45E+12	1.76E+12	1.49E+12	5.94E+11

5.3 Results with Known Experiment Values

This section compares the measurement results with the calculated results. Emphasis is also given here to tunable parameters and adjustments made once the analysts were able to compare measurement with modeling.

When the measurements were first made available, the result differences between the measurements and the Monte Carlo derived results had a bias of ~20-30%. Three perturbations were made to the measurement data after they were compared. First, there was tuning of a photon attenuation correction factor that is calculated using MCNP to aid the measurement process in knowing the fraction of photons that are able to escape the fission wire. The adjustment of this parameter was obtained by adjusting the shape of the wire's dimensions to more accurately represent the wire shape. The wire was first modeled by ignoring small chamfers on the edges. This change seemed to reduce the bias for the most part.

The second change made to measurement data was to correct for the fission yields based on the fission source and spectrum. Initially, the measurement values were calculated assuming the number of fissions had been sourced from thermal U-235 fission. A calculation in Serpent provided a relative contribution of the fissions to distinguish the source between U-235 and U-238 and the spectrum (thermal, epithermal and fast). These relative contributions were then applied to the measured data with their respective fission yields. The epithermal fission yields were assumed to be an average between the thermal and fast yields. An example of the relative fission source is given in Table 19 below.

Table 19. Relative Fission Source.

	Fisson Sources in % of Total Fission					
	U235			U238		
	Thermal	Epithermal	Fast	Thermal	Epithermal	Fast
Position A	41.19	23.00	3.09	0.00	0.07	32.57
Position B	67.31	14.11	1.59	0.00	0.05	16.89
Position C	71.19	12.82	1.39	0.00	0.05	14.52
Position D	65.46	14.83	1.69	0.00	0.06	17.92
Position E	42.13	22.80	3.03	0.00	0.07	31.87

The third change for the measurement data was to use more gamma peaks in the estimation of the total fissions. Below, in Figure 15, the measurement data show the estimated fissions per gram of U-235 based on the isotope peak. From these results, it is clear that there are some issues with Nd-147 at the 531 keV peak, and there is a bias in the I-131 634 keV peak values. It was suspected that the Nd peak has contributions from other isotopes, which over inflated the results for the 1.5% and 2.6% data. This effect can be seen in the two LLSS counts. By comparing the LLSS 1st and 2nd counting, it is observed that the Nd reduced to normal levels from the first to second count. This means that the added isotope was fairly short-lived, and, in order to use Nd-147 as another estimate, the time when the counting takes place after the irradiation is very important. Additionally, it is possible to observe that the I-131 is biased lower by ~10% consistently for all measurements. It is believed that the lower count is due to the fact that I-131 can be a gas and can escape from the fission wire before the measurement of the peak is taken. For these reasons, Nd-147 and I-131 data were removed from contributing to the final measurement data.

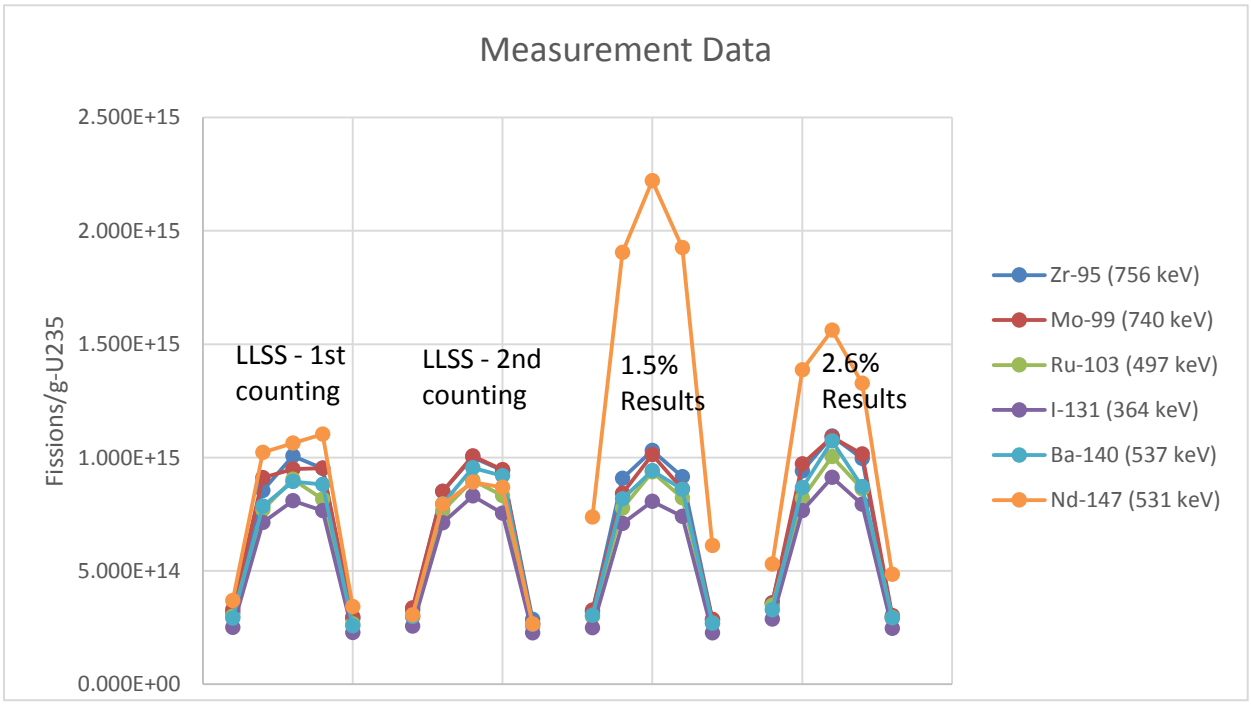

Figure 15. Measurement data from spectral indices.

One of the tunable parameters on the modeling side is the adjustment of the fission energy deposited. Theoretically, there is ~200MeV of energy in a single fission event. However, not all of the energy is deposited in the core. The value of actual fission energy deposited changes from reactor core to reactor core. Acceptable values for the fission energy deposition are between 172 to 200 MeV/fission. This is a spread of ~16%. There is some evidence to suggest the fission energy deposition is ~180 MeV/fission for TREAT and may truly have a spread based on what is going on in the run and length of time. However, the reality is that the analyst has no defensible data to say exactly what the value should be for TREAT or how the fission energy deposition should be determined. For all of the modeling data presented, the fission energy deposition has stayed at 180 MeV/fission for Serpent results and 180.9 MeV/fission for the MCNP results. Even though the fission energy deposition was kept constant for the analysis, it is important to note that ~16% variation could be applied to the results by merely adjusting this parameter.

Both modeling and measurement have quite some latitude with the energy term. For modeling, the energy term is sensitive to starting reactivity and the feedback equation. In reality, the feedback equation is subject to the same question of how well the energy term is known. Thus, they are not independent of each other. From Section 5.2.3, it is possible to see that the energy term could be varied by up to 9.5% for the 2.6% clipped transient. The energy term for the 1.5% transient on the other hand, could only be varied by up to 4%. For measurement, the energy term is dependent on the channels used to classify the core energy. There are three energy channels used to indicate power. However, the only difference between these channels and the other transient detector systems is the circuity that integrates the charge to infer the core energy. The energy channels are even calibrated in the linear mode which is identical to the transient linear channels. The channels not only have a variation in the measured energy value, but, as of this moment, the uncertainties and bias associated with the heat balance process are unknown. In other words, one is forced to accept the detector readings as fact without knowledge of the accuracy, bias, and obvious large variation between estimates.

5.3.1 LLSS Irradiation

Table 20 has the measured fissions per gram of U-235 results from each of the estimators and the average.

Table 20. LLSS Measurement of Fissions per gram of U235.

	LLSS (fissions/g-U235)				
	Position A	Position B	Position C	Position D	Position E
Zr-95 (756 keV)	2.85E+14	9.43E+14	1.00E+15	8.51E+14	3.26E+14
Zr-95 (2σ)	1.47E+13	5.02E+13	5.37E+13	4.40E+13	1.77E+13
Mo-99 (740 keV)	2.67E+14	9.46E+14	1.01E+15	8.50E+14	3.36E+14
Mo-99 (2σ)	2.79E+13	9.75E+13	1.04E+14	8.33E+13	3.48E+13
Ru-103 (497 keV)	2.54E+14	8.31E+14	9.00E+14	7.65E+14	2.96E+14
Ru-103 (2σ)	1.40E+13	5.06E+13	5.64E+13	4.62E+13	1.67E+13
Ba-140 (537 keV)	2.64E+14	9.20E+14	9.54E+14	7.95E+14	2.98E+14
Ba-140 (2σ)	1.35E+13	4.89E+13	5.16E+13	4.18E+13	1.58E+13
Average	2.68E+14	9.10E+14	9.66E+14	8.15E+14	3.14E+14
Average (2σ)	1.86E+13	6.52E+13	7.00E+13	5.65E+13	2.27E+13

The determination of the energy from the LLSS irradiation was discussed in Section 5.2.1 with as-run data. The DIS-chamber energy is taken as 593.6 MJ, while the best estimate for the true actual energy is taken as 599.6 MJ. Table 21 compares the measured results with the best estimated simulation data. The measured PCF values used the best estimate of the energy and the average measurement values. The comparison between the Serpent model results and the measurement seemed to have the best agreement, with the exception of Position B. Comparing the MCNP model predictions with the measurement value shows a constant bias of ~ −9%, except for Position B. It is suspected that there is some issue with the measurement value in Position B, given that the rest of the positions tend to be consistent.

Table 21. LLSS PCF Comparison.

	LLSS (f/g-U235-MJ)				
	Position A	Position B	Position C	Position D	Position E
Serpent - As Run	4.53E+11	1.33E+12	1.57E+12	1.26E+12	5.10E+11
MCNP - As Run	4.90E+11	1.44E+12	1.77E+12	1.48E+12	5.73E+11
Avg Measurement	4.46E+11	1.52E+12	1.61E+12	1.36E+12	5.24E+11
	Differences %				
Serpent vs Measurement	-1.43%	12.56%	2.57%	6.96%	2.56%
MCNP vs Measurement	-9.83%	4.85%	-9.72%	-8.89%	-9.41%

5.3.2 1.5%Δk/k Natural Transient

Table 22 has the measured fissions per gram of U-235 results from each of the estimators and the average.

Table 22. 1.5% Measurement of Fissions per gram of U235.

	1.5% (fissions/g-U235)				
	Position A	Position B	Position C	Position D	Position E
Zr-95 (756 keV)	2.84E+14	9.16E+14	1.03E+15	9.08E+14	3.19E+14
Zr-95 (2σ)	1.61E+13	5.37E+13	6.00E+13	5.19E+13	1.45E+13
Mo-99 (740 keV)	2.85E+14	8.62E+14	1.01E+15	8.42E+14	3.26E+14
Mo-99 (2σ)	1.83E+13	5.86E+13	6.76E+13	5.62E+13	1.73E+13
Ru-103 (497 keV)	2.69E+14	8.22E+14	9.36E+14	7.77E+14	2.97E+14
Ru-103 (2σ)	1.55E+13	5.28E+13	6.14E+13	5.02E+13	1.55E+13
Ba-140 (537 keV)	2.69E+14	8.60E+14	9.42E+14	8.17E+14	3.03E+14
Ba-140 (2σ)	1.41E+13	4.73E+13	5.22E+13	4.48E+13	1.38E+13
Average	2.77E+14	8.65E+14	9.80E+14	8.36E+14	3.11E+14
Average (2σ)	1.61E+13	5.33E+13	6.06E+13	5.10E+13	1.53E+13

A summary of the reported and calculated energy values based on the ARCS data and reactivity computer are provided below. The signal for the RTS-Transient-Log A to the reactivity computer is not behaving appropriately to a reasonable degree to be believable at the moment. The simulated energy values for this transient varied from 583.4 to 595.7 MJ, with an additional 7.02 MJ being added afterward to account for the energy deposited before the transient began. As can be seen from Table 23, the possible measured energy values varied from 443 to 576.7 MJ (30% variation). The values in the table ignore the energy before the transient. The simulated energy values were just a little higher than any of the energy values, but this does not mean that the simulated results are wrong given the uncertainty in the energy determination process. The average from the energy chambers gives 568.2 +/− 11.5 MJ.

Table 23. 1.5% Measured Energy Values.

	RTS Linear A	RTS Linear B	RTS Linear C	RTS Log A	RTS Log B	RTS Log C
ARCS Data - Energy (MJ)	442.9	488.4	529.8	506.4	502.6	491.9
Rx Computer - Energy (MJ)	567.0	561.4	560.5	NA	547.5	496.7
	RTS Energy A	RTS Energy B	RTS Energy C	ARCS Linear	ARCS Log	
ARCS Data - Energy (MJ)	576.7	572.8	555.2	554.7	555.7	—
Rx Computer - Energy (MJ)	575.9	572.4	554.4	557.8	521.2	—

It is difficult to say with great certainty what the true energy value is. It is possible to compare the total fissions per gram of U-235 and ignore dividing by the core energy. In this case, the true energy term is imbedded with the actual measurement value since the integral fissions are a result of the total core energy. In this case, the energy for the simulation could be manipulated or chosen at will.

The results of the integral fissions per gram of U235 are compared in Table 24 with the simulation result, assuming 595.92 MJ from the 1.5% reactivity case with 7.02MJ in Section 5.2.2 and 568.2 MJ from the average energy detector in Table 23. It is easy to see that going to energies above 595.92 MJ is better for the Serpent model results, while 568.2 MJ is just about right for the MCNP data.

Hypothetical core energies were also calculated to make the simulation vs. measurement data become centered about the 0% line. The data are found in Table 25. The best fit energies were 629.8 MJ for the Serpent model and 568.45MJ for the MCNP model. The MCNP best fit energy happens to be nearly identical to the average of the RTS-Energy channels. The best fit energy for the Serpent model exceeds all simulated and measured values, thus concluding that the results would end up with a bias, albeit 5%, if the simulation prediction of 595.92 MJ is correct and 11% if the average RTS-Energy channel is correct.

Table 24. 1.5% Comparison of model results assuming core energy.

1.50%	Fissions/(g-U235)				
	Position A	Position B	Position C	Position D	Position E
Serpent (Assume 595.92 MJ)	2.68E+14	7.89E+14	9.37E+14	7.59E+14	3.07E+14
MCNP (Assume 595.92 MJ)	2.86E+14	8.60E+14	1.04E+15	8.67E+14	3.46E+14
Serpent (Assume 568.2 MJ)	2.56E+14	7.52E+14	8.93E+14	7.24E+14	2.93E+14
MCNP (Assume 568.2 MJ)	2.73E+14	8.20E+14	9.94E+14	8.27E+14	3.30E+14
Avg Measurement	2.77E+14	8.65E+14	9.80E+14	8.36E+14	3.11E+14
	% Differences				
Serpent (595.92 MJ) vs Measurement	-3.07%	-8.78%	-4.43%	-9.14%	-1.46%
MCNP (595.92 MJ) vs Measurement	3.46%	-0.57%	6.29%	3.77%	11.20%
Serpent (568.2 MJ) vs Measurement	-7.58%	-13.03%	-8.88%	-13.37%	-6.05%
MCNP (568.2 MJ) vs Measurement	-1.35%	-5.19%	1.35%	-1.06%	6.03%

Table 25. Hypothetical Core Energies to make data center about 0% difference.

1.50%	Best Fit Core Energy [fissions/(g-U235)]				
	Position A	Position B	Position C	Position D	Position E
Serpent (Assume 629.8 MJ)	2.83E+14	8.34E+14	9.90E+14	8.03E+14	3.24E+14
MCNP (Assume 568.45 MJ)	2.73E+14	8.20E+14	9.94E+14	8.27E+14	3.30E+14
	% Differences				
Serpent (629.8 MJ) vs Measurement	2.44%	-3.60%	1.00%	-3.98%	4.14%
MCNP (568.45 MJ) vs Measurement	-1.30%	-5.15%	1.39%	-1.01%	6.08%

5.3.3 2.6%Δk/k Clipped Transient

Table 26 has the measured fissions per gram of U-235 results from each of the estimators and the average.

Table 26. 2.6% Measurement of Fissions per gram of U235.

	2.6% (fissions/g-U235)				
	Position A	Position B	Position C	Position D	Position E
Zr-95 (756 keV)	2.92E+14	9.96E+14	1.09E+15	9.41E+14	3.59E+14
Zr-95 (2$\boldsymbol{\sigma}$)	1.74E+13	5.82E+13	6.33E+13	5.28E+13	2.04E+13
Mo-99 (740 keV)	3.02E+14	1.02E+15	1.09E+15	9.71E+14	3.58E+14
Mo-99 (2$\boldsymbol{\sigma}$)	2.15E+13	7.41E+13	7.87E+13	6.67E+13	2.50E+13
Ru-103 (497 keV)	2.94E+14	8.62E+14	1.00E+15	8.20E+14	3.48E+14
Ru-103 (2$\boldsymbol{\sigma}$)	1.71E+13	5.56E+13	6.55E+13	5.24E+13	1.99E+13
Ba-140 (537 keV)	2.92E+14	8.71E+14	1.07E+15	8.67E+14	3.28E+14
Ba-140 (2$\boldsymbol{\sigma}$)	1.56E+13	4.88E+13	5.87E+13	4.71E+13	1.75E+13
Average	2.95E+14	9.36E+14	1.07E+15	9.00E+14	3.48E+14
Average (2$\boldsymbol{\sigma}$)	1.80E+13	5.99E+13	6.70E+13	5.53E+13	2.09E+13

A summary of the reported and calculated energy values based on the ARCS data and reactivity computer is provided below. The signal for the RTS-Transient-Log A to reactivity computer is not behaving appropriately to a reasonable degree to be believable at the moment. The simulated energy values for this transient varied from 588.9 to 644.7 MJ, with the most probable being 628.4 MJ, and an additional 4.9 MJ being added afterward to account for the energy deposited before the transient began. As can be seen from Table 27, the possible measured energy values varied from 545 to 630 MJ (15% variation). The values in the table ignore the energy before the transient. The simulated energy values were just a little higher than any of the energy values, just as was observed in the 1.5% transient. This does not mean that the simulated results are wrong or biased given the uncertainty in the detector calibration process. The average from the energy chambers gives 616.7 +/− 9.2 MJ.

Table 27. 2.6% Measured Energy Values.

	RTS Linear A	RTS Linear B	RTS Linear C	RTS Log A	RTS Log B	RTS Log C
ARCS Data - Energy (MJ)	582.2	584.5	611.7	552.3	560.5	546.0
Rx Computer - Energy (MJ)	618.9	596.5	630.0	NA	597.6	580.4
	RTS Energy A	RTS Energy B	RTS Energy C	ARCS Linear	ARCS Log	
ARCS Data - Energy (MJ)	621.5	622.4	606.0	590.1	594.2	—
Rx Computer - Energy (MJ)	620.2	615.7	602.4	587.1	544.6	—

It is difficult to say with great certainty what the true energy value is. It is possible to compare the total fissions per gram of U-235 and ignore dividing by the core energy. In this case, the true energy term is imbedded within the actual measurement value since the integral fissions are a result of the total core energy. In this case, the energy for the simulation could be manipulated or chosen at will.

The results of the integral fissions per gram of U235 are compared in Table 28 with the simulation results using the best estimate from the simulation and the average of the energy detectors. From the data, it is easy to see that going to energies above the simulation energy is better for the Serpent model results, while the average detector energy is just about right for the MCNP data.

Hypothetical core energies were also calculated as was done for the 1.5% data to make the simulation vs. measurement data become centered about the 0% line. The best fit energies were 681.24 MJ for the Serpent model and 610.53 MJ for the MCNP model. The MCNP best fit energy happens to be nearly identical to the average of the RTS-Energy channels. The best fit energy for the Serpent model exceeds all simulated and measured values, thus concluding that the results would end up with a bias, albeit 7.5%, if the simulation prediction of 633.3 MJ is correct and 10.4% if the average RTS-Energy channel is correct.

Table 28. 2.6% Comparison of model results assuming core energy.

	fissions/(g-U235)				
	Position A	Position B	Position C	Position D	Position E
Serpent (Assume 633.3MJ)	2.82E+14	8.39E+14	1.00E+15	8.12E+14	3.33E+14
MCNP (Assume 633.3 MJ)	3.04E+14	9.17E+14	1.12E+15	9.45E+14	3.76E+14
Serpent (Assume 616.7 MJ)	2.74E+14	8.17E+14	9.77E+14	7.91E+14	3.24E+14
MCNP (Assume 616.7 MJ)	2.96E+14	8.93E+14	1.09E+15	9.20E+14	3.66E+14
Avg Measurement	2.95E+14	9.36E+14	1.07E+15	9.00E+14	3.48E+14
	% Differences				
Serpent (633.3MJ) vs Measurement	-4.48%	-10.32%	-6.24%	-9.76%	-4.38%
MCNP (633.3MJ) vs Measurement	3.21%	-2.07%	4.45%	4.95%	8.10%
Serpent (616.7MJ) vs Measurement	-6.99%	-12.67%	-8.70%	-12.12%	-6.89%
MCNP (616.7 MJ) vs Measurement	0.51%	-4.64%	1.72%	2.20%	5.27%

5.3.4 Additional Model Results and Intra-Run Results

One of the goals of the ATF-3-1 transient prescription was to answer the question of whether the PCF value would change significantly depending on the run histories if the integral power was identical. For this reason, the LLSS, 1.5% natural transient and the 2.6% clipped transient were designed to each produce about 576MJ. Even though it is not possible to obtain exactly this amount of energy for each run, they were designed to get as close as possible. The simulation and measured PCF results are presented below in Table 29 and in Figures 16-18. Figures 19-21 show the differences between the model results and the measurement values. Two additional models were employed. The first addition was another MCNP model that was developed by Argonne National Laboratory (ANL) for TREAT before it was put on standby status. This new MCNP model will be referred to as MCNP-ANL. The second additional model used the MAMMOTH code. MAMMOTH is a 3-D, time dependent code, and the modeling methods were outlined in Section 3.2.

The PCF values for the simulations were produced using the simulation energy from RELAP5-3D if it was a Monte Carlo-based code while MAMMOTH used its own developed power history. The measured PCF values were calculated using the average RTS-energy channel data for the transients and the DIS-Linear channel data for the LLSS. MAMMOTH was not used to perform an LLSS calculation due to time constraints. Keep in mind that the measurement value is assuming an energy based on the detector systems. It has been explained in prior sections that this value is not very defendable and only represents the best estimate. The figures showing the difference between the calculation and measurement PCF values are only with respect to the chosen energy. The true energy could cause the graphs to shift up or down by up to ~20%.

Table 29. Intra-Run PCF results.

	Measured PCF (fissions/g-U235-MJ)					
	Position A	Position B	Position C	Position D	Position E	Energy (MJ)
LLSS	4.51E+11	1.53E+12	1.63E+12	1.37E+12	5.29E+11	593.6
1.50%	4.87E+11	1.52E+12	1.73E+12	1.47E+12	5.48E+11	568.2
2.60%	4.78E+11	1.52E+12	1.73E+12	1.46E+12	5.64E+11	616.7
	Serpent PCF (fissions/g-U235-MJ)					
	Position A	Position B	Position C	Position D	Position E	Energy (MJ)
LLSS	4.53E+11	1.33E+12	1.57E+12	1.26E+12	5.10E+11	599.6
1.50%	4.50E+11	1.32E+12	1.57E+12	1.27E+12	5.15E+11	595.92
2.60%	4.45E+11	1.33E+12	1.58E+12	1.28E+12	5.25E+11	633.3
	MCNP PCF (fissions/g-U235-MJ)					
	Position A	Position B	Position C	Position D	Position E	Energy (MJ)
LLSS	4.90E+11	1.44E+12	1.77E+12	1.48E+12	5.73E+11	599.6
1.50%	4.80E+11	1.44E+12	1.75E+12	1.46E+12	5.81E+11	595.92
2.60%	4.81E+11	1.45E+12	1.76E+12	1.49E+12	5.94E+11	633.3
	MCNP-ANL PCF (fissions/g-U235-MJ)					
	Position A	Position B	Position C	Position D	Position E	Energy (MJ)
LLSS	4.89E+11	1.38E+12	1.59E+12	1.42E+12	5.41E+11	599.6
1.50%	5.01E+11	1.38E+12	1.69E+12	1.41E+12	5.57E+11	595.92
2.60%	4.61E+11	1.37E+12	1.66E+12	1.42E+12	5.71E+11	633.3
	MAMMOTH PCF (fissions/g-U235-MJ)					
	Position A	Position B	Position C	Position D	Position E	Energy (MJ)
LLSS	NA	NA	NA	NA	NA	NA
1.50%	4.92E+11	1.49E+12	1.79E+12	1.45E+12	5.68E+11	612
2.60%	4.97E+11	1.50E+12	1.80E+12	1.46E+12	5.72E+11	903.5

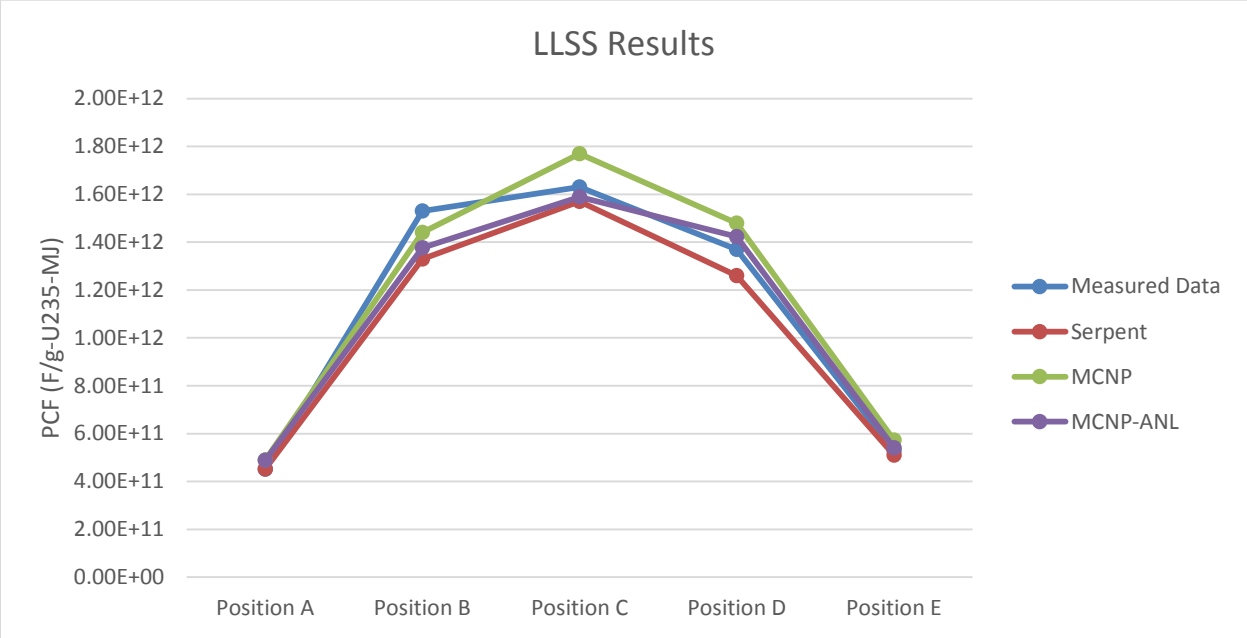

Figure 16. LLSS Results (Models and Measurement).

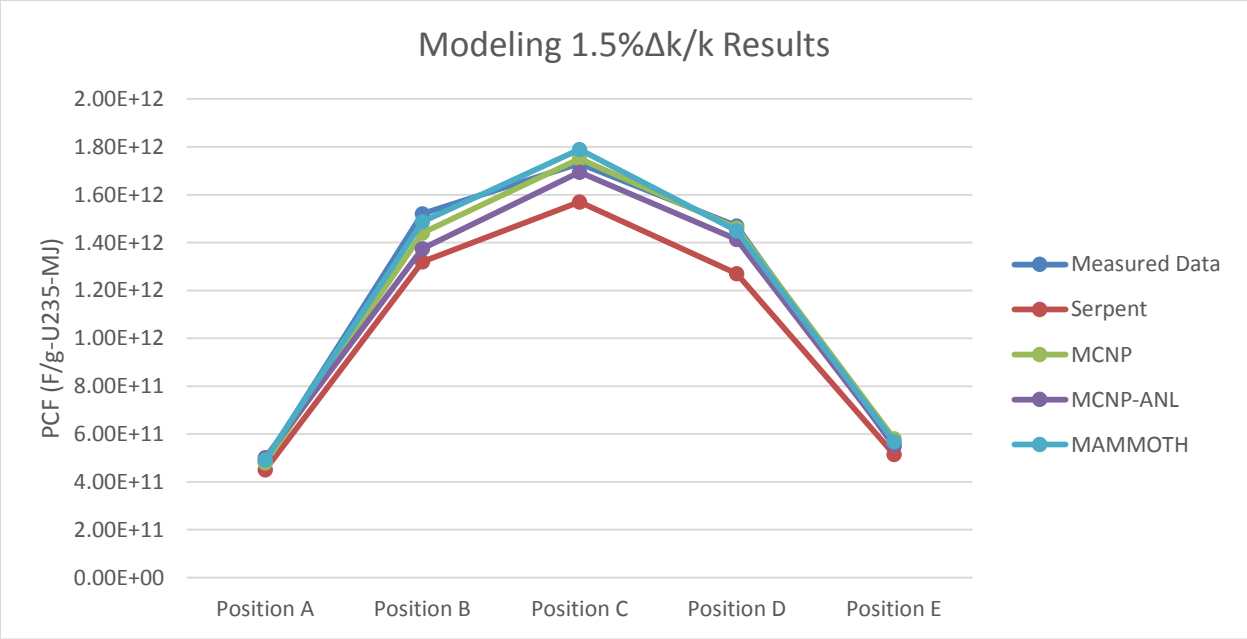

Figure 17. 1.5%dk/k Results (Models and Measurement).

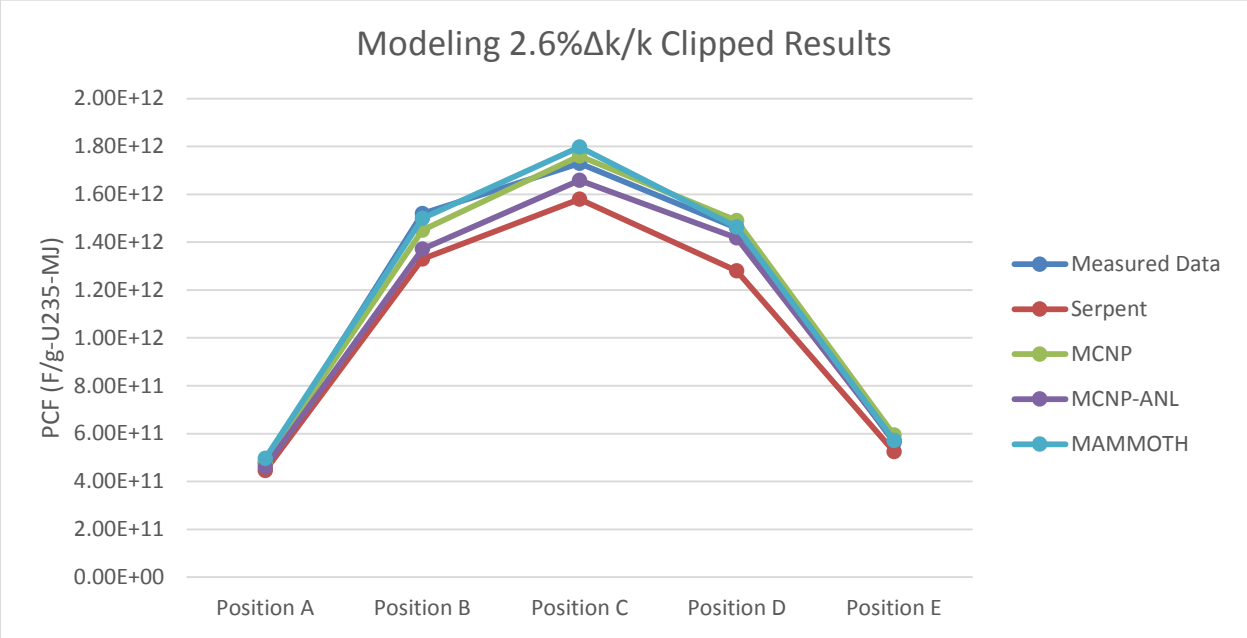

Figure 18. 2.6% dk/k Clipped Results (Models and Measurement).

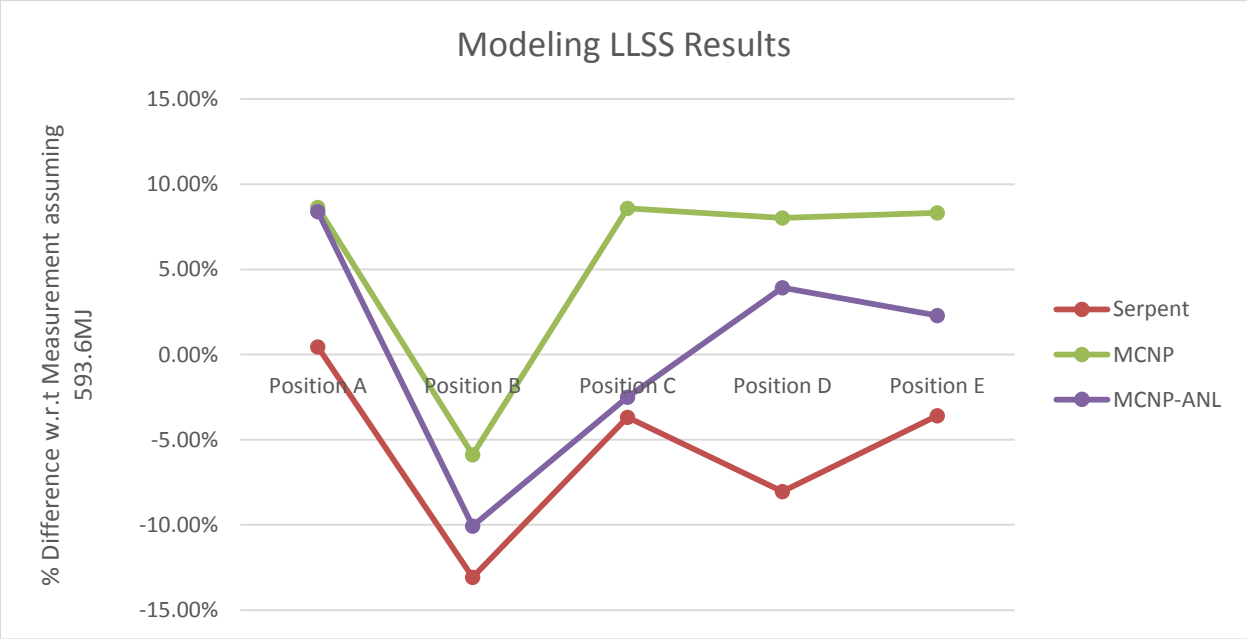

Figure 19. Relative percent differences for LLSS results.

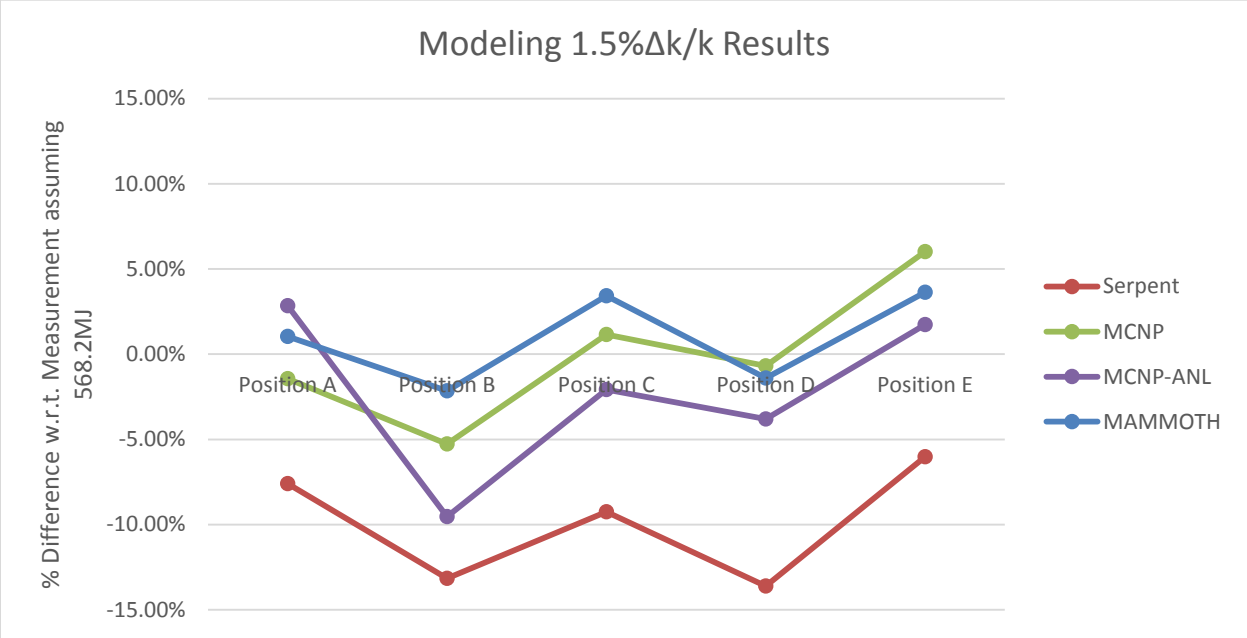

Figure 20. Relative percent differences for 1.5%dk/k results.

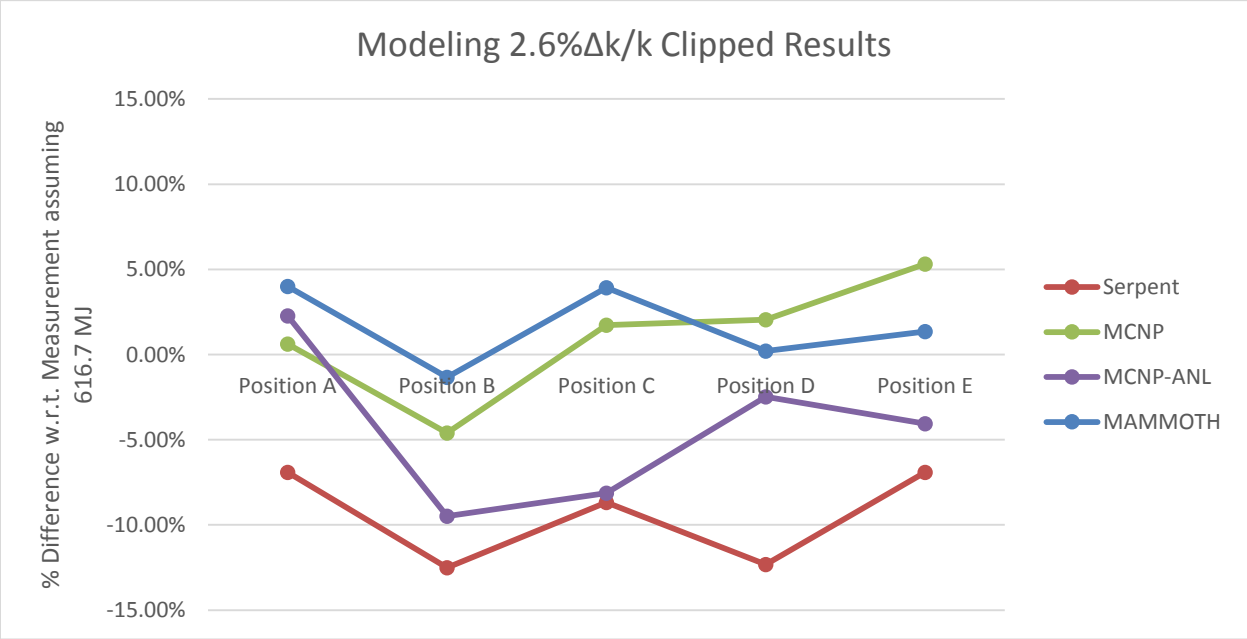

Figure 21. Relative percent differences for 2.6%Δk/k clipped results.

Analyzing the modeling data between Monte Carlo type solutions shows that there is ~15 to 20% change in the results based on the model used. This is most likely due to the inherent differences that come about from models being developed by different people and the assumptions that they make. Further analysis of the models could reduce the differences, but do not necessarily imply correctness.

The MAMMOTH model seemed to perform very well in comparison with the measured results for this particular choice of deposited energy. However, the MAMMOTH model transient history showed that the period was significantly different than the recorded value. The recorded value was ~9 sec^{-1} which corresponds to ~1.5%Δk/k and the MAMMOTH simulation was producing ~10 sec^{-1} which corresponds to ~1.55%Δk/k. Due to the incorrect period, the MAMMOTH model did not match very well with measured energy. Further analysis is needed to reduce the power prediction difference between the model and measurement histories. Adjustment of the reactivity is significantly different between the point kinetics method and the 3-D diffusion method used by MAMMOTH. MAMMOTH used reported rod movements to generate the transient while point-kinetics can simply specify the desired reactivity or a corresponding rod position to create the reactivity. However, the trade-off is that MAMMOTH does a
3-D transient and can be coupled to additional physics to serve the experiment region while point kinetics represents the global core behavior in a single power value and various factors like the PCF are required to couple to experiment calculations.

The spread in the differences for MAMMOTH data was consistently ~5.8% which was lower than all other models and might be due to the inclusion of 3-D effects such as the temperature profile, which is constant for the Monte Carlo methods. Serpent had a spread of 5 to 13.5%, the MCNP model had a spread of 10 to 14.5%, and the MCNP-ANL model had a spread of 11.8 to 18.5%.

Comparison of the measured PCF results for all runs showed a variation of less than 8%. The lowest PCF values for the measurement results were consistently in the LLSS data, while the transient results were nearly identical. The reason for this discrepancy is most likely due to the requirement to change the method of energy determination between a steady state operation and a transient operation. The simulation results show a change of less than 6% for any of the positions and for a given model.

The measurement and calculation data seem to agree fairly well with the conclusion that there is not any significant change in the PCF factor when the history of the run changes significantly.

5.4 Overview of Modeling & Measurement Stages

Overall, it was clear from data analysis stages that not much changed from the as-run data from the initial PCF estimates, if the correct enrichment had been known at the time. Thus, the blind predictions were fairly good estimates but would have increased the difference by a few percent. There were a few measurement calculations and processes changed once the measurements were compared with the simulated data. Given the uncertainty in the fission energy deposition value, the core energy term and photon attenuation in the counting, there is truly a range of uncertainty of ~20% when comparing simulation results with measurement. It is assumed that the best-estimated values were chosen for the analysis, and the results were presented in Section 5.3.

Some of the takeaways form the results include that the Serpent model performed rather well for the LLSS irradiation but seemed to require a higher energy than might have been possible for the transients. The MCNP model had a bias of ~9% for the LLSS but seemed to match very well using the average energy detector reading. One of the potential reasons for the difference in consistency between the LLSS and transients has to do with using two different detector types. Steady state operations require chambers that are closer to the core for a better signal, while the transient detectors are barely registering at 20kW, since they are very far away, which produces challenges in making the detectors read the same values for a heat balance. Further, the calibration between the chamber reading and the true core power is non-linear and depends on core physics. This is more pronounced in the steady state chambers. Finally, the accuracy of the detector calibration process (i.e., heat balance) is completely unknown at this moment, with only minor observations and inadequate amounts data for substantive quantification of the bias and uncertainty. From an operational standpoint, the core power for TREAT does not really need to be known since the limiting condition of TREAT's operation is the core temperature. From an experimental point of view, it is beneficial to have more confidence in the core energy term. However, even without the confidence, it is possible to maintain consistency if a single channel is chosen as a reference, but the values no longer apply when trying to compare with modeling results.

6. NPW Transient Prescription Tests, Data Results

It is of interest in the LWR community to alter TREAT operations to minimize the pulse width during transients to more closely match expected values of full-width half-maximum (FWHM) during HZP-RIA. TREAT historically performed many clipped transients (approximately fifty) by initiating a temperature limited transient and reinserting the transient control rods near the peak power point of pulse, but none of these transients were optimized for a minimum pulse width where the transient rods should be re-inserted moments prior to the peak power. The previously-described NPW transient prescription tests were intended to accomplish the express purpose of determining TREAT's most-narrow pulse capability in the M8 half-slot core configurations. All of the MPW transients were initiated with a step change in reactivity of 4.2% Δk/k, but varied the clipping delay time in each transient. As the clipping delay increased, a larger peak power and energy released were achieved. When the clipping delay time was increased further, the transient behaved more like a temperature limited transient. These transients were the first TREAT operations ever to achieve a FWHM less than 100 milliseconds (ms), and the key results are shown in Table 30.

One issue of concern was the repeatability of transient rod motions in TREAT. There are eight transient control rods, divided into four rod drives with two rods per drive. Each drive may respond differently. As can be seen in Figure 22, the control rod drives moved at slightly different rates during ejection out of and insertion into the core. However, it was found that for all transients operated with clipping, the rod motions were repeatable and nearly identical to each other. This observation demonstrates that transient rod acceleration, although not identical between drives, is repeatable and can be accounted for in transient prescription programming. The transients listed in Table 30 are compared in Figure 23 to illustrate the effect of rod position and clipping delay time on the peak power and transient shape. Finally, Figure 24 provides the energy released and FWHM as a function of clipping delay time. As expected, a longer delay time for clipping resulted in increased energy released. A minimum of 89 ms FWHM was achieved in TREAT with a clipping delay time of approximately 475 ms.

Table 30. Summary of NPW transients.

Transient	Reactivity Insertion (%Δk/k)	Peak Power[a] (MW)	Total Energy Released[b] (MJ)	Clipping Delay Time (ms)	Pulse Width (FWHM) (ms)	Date
2904	4.2	8840	949	475	89	07/03/2018
2905	4.2	11178	1209	500	90	07/11/2018
2906	4.2	12277	1327	513	90	07/12/2018
2907	4.2	13240	1451	525	92	07/17/2018
2908	4.2	5758	643	450	92	07/19/2018

a. Peak power based on RTS Transient Linear A channel
b. Energy Released as reported by the RTS Transient Energy A channel

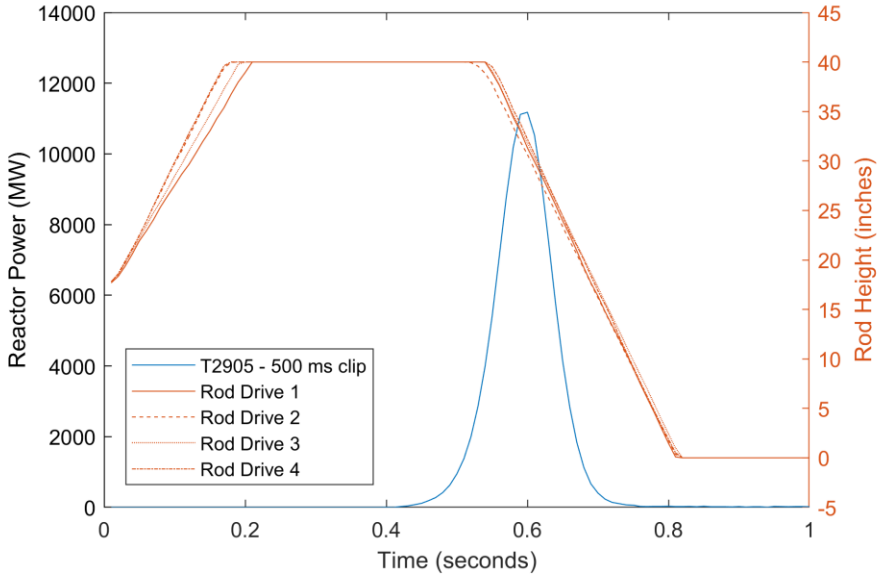

Figure 22. Reactor power and rod position during transient 2905.

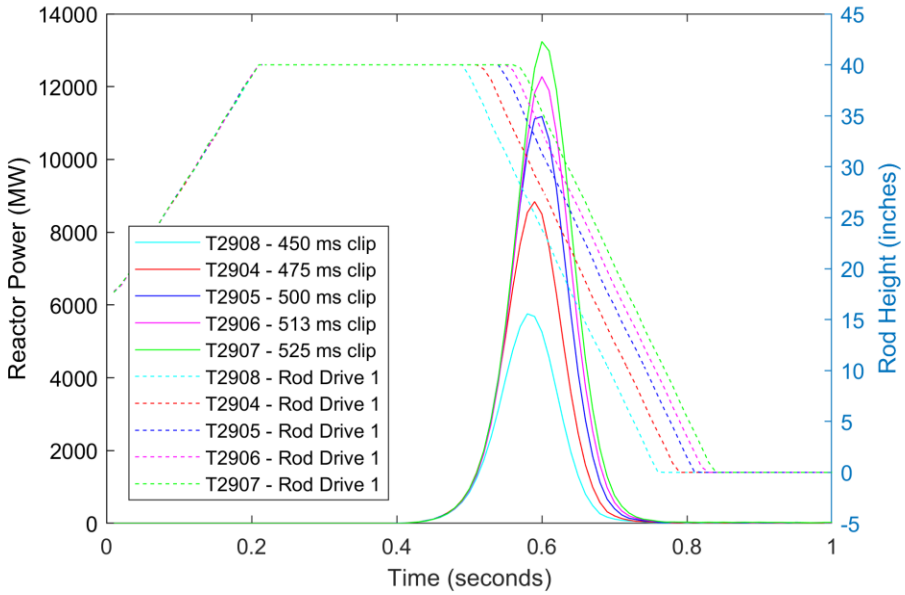

Figure 23. Reactor power and rod position during various clipped transients.

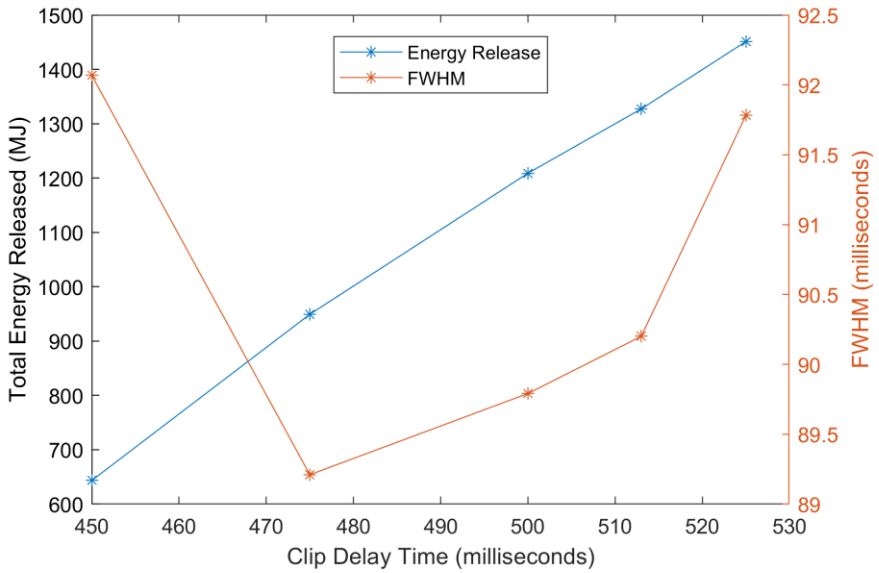

Figure 24. Energy released and FWHM as function of clip delay time.

7. LOCA Transient Prescription Tests, Data Results

TREAT is also capable of simulating LOCA events by operating steadily at an elevated power level for a long period of time and then rapidly inserting the control rods and operating steadily at a lower power level. These types of power shapes are accomplished by an active feedback reactor control system which manipulates transient rod positions based on reactor instrumentation. Two transients, transients 2902 and 2903, were performed in TREAT to demonstrate the repeatability of this capability. While similar "flattop" transients were performed historically, this precise power shape, which was focused on full LOCA simulation, had not been performed previously. Table 31 presents characteristics of the LOCA transients 2902 and 2903. The peak power during the steady elevated power level did not exceed 47.5 MW, and the total energy released for each transient was approximately 2100 MJ. The duration of elevated power for each transient was approximately 30 seconds and approximately 195 seconds for the low power operations. Figure 25 and Figure 26 provide the reactor power and energy released, respectively, as a function of time for transient 2902. Additionally, each plot contains the rod motion as a function of time to illustrate the reactor operations required to obtain the simulated LOCA transient. Only the rod motion for drive 1 is reported. However, all transient control rod drives are maneuvered similarly. The data obtained from transient 2903 are nearly identical to transient 2902 and are not presented.

As can be observed in Figure 25, due to temperature increase in the reactor while operating, the transient control rods must be withdrawn following the change to low power level operations. However, once the transient control rods are fully withdrawn to their maximum height of 40 inches, the negative reactivity associated with elevated temperature becomes dominant, and the reactor power decreases until the transient is terminated.

Table 31. Summary of LOCA Transients.

Transient	Peak Power[a] (MW)	Total Energy Released[b] (MJ)	Duration at elevated power (sec)	Duration at low power (sec)	Date
2902	47.5	2113	30	195	06/26/2018
2903	47.4	2141	30	195	06/27/2018

a. Peak power based on RTS Transient Linear A channel
b. Energy Released as reported by the RTS Transient Energy A channel

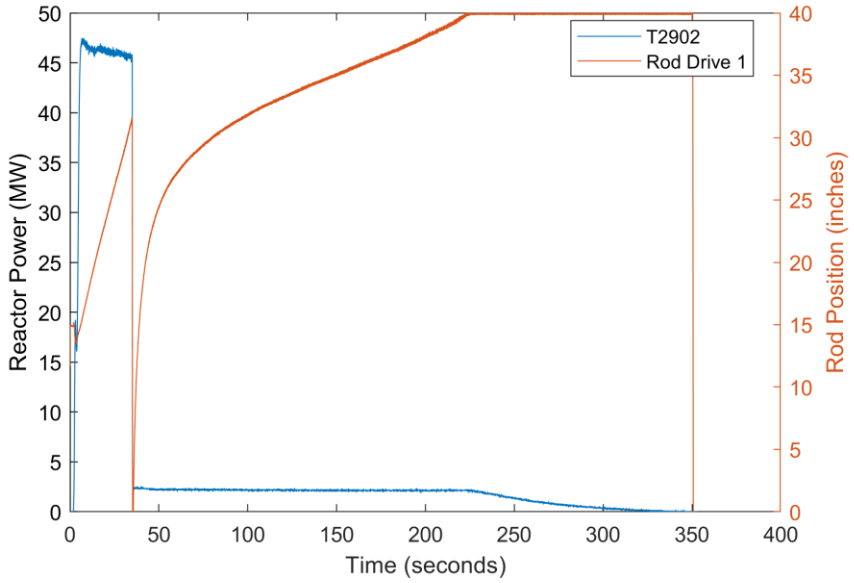

Figure 25. Reactor power and rod position during transient to simulate LOCA.

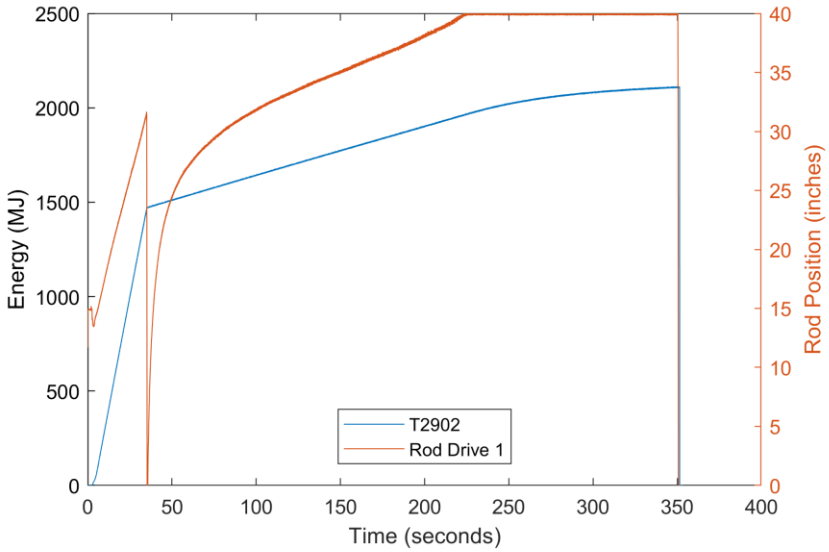

Figure 26. Energy released and rod position during transient to simulate LOCA.

8. CONCLUSIONS

The ATF-3, NPW, and LOCA transient prescription tests were successfully carried out in TREAT. The ATF-3 transient prescriptions consisted of one LLSS irradiation, a 1.5% natural transient, and three 2.6% clipped transients, all which were design to release approximately the same amount of reactor energy. The three clipped transients were performed to establish the repeatability of the transient process, and all metrics indicate that TREAT is very repeatable to within a few percent. Uranium fission wires were irradiated in one of each of these three types of reactor operations to establish if the PCF changed drastically between the run types. The measurement and modeling results both showed that the PCF factor does not change by any more than 8% between the three runs types.

Additionally, modeling evolution steps were presented, and final results were compared with measurement values for each run type. The modeling stages proved to hardly change using as-run data and blind predictions. Using the best estimated values for the measurement energy and modeling results, the models to measurement differences tended to have variations of ~6-15% in the data spread. The maximum and minimum differences went from -13 to 13%, with the average being much smaller. A bias of up to 16% existed between the Monte Carlo models. Potential biases could exist between the data and models but could not be determined to any significant degree given the potential variation in adjustable parameters.

The fission energy deposition and core energy were identified as two of the largest tunable parameters for the simulation results, with potential spreads of ~20%. Additional sensitive factors, such as the photon attenuation, were identified in the measurement method to change the results by over 20% as well. Further investigation is needed to reduce these tunable parameters, such as using mass spectrometry to better characterize the measurement result. Overall, the ATF-3 transient prescription tests were successful in determining repeatability and consistency of the PCF factor, developing processes for modeling and measuring this crucial parameter, and demonstrating the need for continued efforts in transient prescription work at TREAT in support of future experiment design and post test data interpretation.

Similarly, the NPW and LOCA transient prescriptions were performed to exhibit TREAT's capability for these important LWR accident categories. Both NPW and LOCA transients successfully demonstrated these transient shapes, neither of which had ever been performed historically. The NPW transients showed pulse widths of ~90 ms, which is relevant for the upper end range of HZP-RIA simulation, while providing crucial data for calibrating kinetic models to be used in enhanced pulse-narrowing strategies to be used in upcoming irradiations. The LOCA transient prescriptions showed that TREAT can simulate the needed nuclear heating and event time scales for LOCA fuel safety research and provided essential data for future experiment design.

9. REFERENCES

1. ATF 3-1 Transient Prescription Data Package, INL Internal Document DP-125, rev 1, 03/20/2018.
2. Narrow Pulse Width Transients Data Package, INL Internal Document DP-126, rev 0, 02/08/2018.
3. LOCA Transient Prescription Study Data Package, INL Internal Document DP-128, rev 0, 05/30/2018.
4. W.R. Robinson, T.H. Bauer, The M8 Power Calibration Experiment (M8CAL), Tech. Rep. ANL-IFR-232, Argonne National Laboratory (May 1994).
5. Interoffice Memorandum (INL), To David Chichester, From Mathew Snow. Subject: Unirradiated Uranium Wire Mass Spectrometry Analyses for Trace Element and Uranium Isotopics. (CCN 243092) July 11, 2018.
6. INL – Materials and Fuels Complex Analytical Laboratory, AL Log #: 101858, Name: LANL DEPLETED URANIUM WIRES FOR TREAT METROLO, Requester: D. Chichester, May 17, 2018.
7. Determination of DU Wire Enrichment for TREAT Metrology by Gamma Spectroscopy, From Tommy Holschuh, INL Internal Document CCN 243332, Sep 6, 2018.
8. TREAT work order: 253090-01, TREAT 720 Collect Samples Measurements and photos of DU wire
9. TREAT Form: Monitor Wire Holder Configuration Traveler. Experiment Name: ATF-3-1 Transient Prescription, Experiment ID: ATF-3-1-TPSS, ATF-3-1-TP1.5 and ATF-3-1-TP2.6, Holder ID's: T-MWH-001, T-MWH-002, T-MWH-003.

10. F. Gleicher, J. Ortensi, R. Williamson, et al, "The Coupling of the Neutron Transport Application Rattlesnake to the Nuclear Fuels Performance Application BISON under the MOOSE Framework," PHYSOR 2014, November 2014.
11. Y. Wang, S. Schunert, et al, "Rattlesnake Theory Manual", INL external report, INL/EXT-17-42103, April 2018.
12. M. DeHart, B. Baker, "Interpretation of energy deposition data from historical operation of the transient test facility (TREAT)", Nuclear Engineering and Design, vol 322, p. 504-521, 2017.Development and Validation of a Detailed RELAP5-3D Point Kinetics Model of TREAT, INL Internal Document ECAR-3838, rev 0, 09/20/2017.
13. Richard L Williamson et al. "Multidimensional multiphysics simulation of nuclear fuel behavior." Journal of Nuclear Materials, 423: pp. 149 – 163 (2012).
14. Development and Validation of a Detailed RELAP5-3D Point Kinetics Model of TREAT, INL Internal Document ECAR-3838, rev 0, 09/20/2017.